

N O T I C E

THIS DOCUMENT HAS BEEN REPRODUCED FROM
MICROFICHE. ALTHOUGH IT IS RECOGNIZED THAT
CERTAIN PORTIONS ARE ILLEGIBLE, IT IS BEING RELEASED
IN THE INTEREST OF MAKING AVAILABLE AS MUCH
INFORMATION AS POSSIBLE

JPL PUBLICATION 81-38

(NASA-CR-164530) THE 1-KW SOLAR STIRLING
EXPERIMENT Final Report (Jet Propulsion
Lab.) 107 p HC A06/MF A01 CACL 10A

N81-27602

Unclas
G3/44 26796

1-kW Solar Stirling Experiment Final Report

Anthony Glandomenico



May 15, 1981

National Aeronautics and
Space Administration

Jet Propulsion Laboratory
California Institute of Technology
Pasadena, California

JPL PUBLICATION 81-38

1-kW Solar Stirling Experiment Final Report

Anthony Glandomenico

May 15, 1981

**National Aeronautics and
Space Administration**

**Jet Propulsion Laboratory
California Institute of Technology
Pasadena, California**

The research described in this publication was carried out by the Jet Propulsion Laboratory, California Institute of Technology, under contract with the National Aeronautics and Space Administration.

ABSTRACT

The objective of this experiment was to demonstrate electrical power generation using a small free-piston Stirling engine and linear alternator in conjunction with a parabolic solar collector.

A test bed collector, formerly used at the JPL Table Mountain Observatory, was renovated and used to obtain practical experience and to determine test receiver performance. The collector was mounted on a two-axis tracker, with a cold water calorimeter mounted on the collector to measure its efficiency, while a separate, independently tracking radiometer was used to measure solar insolation.

The solar receiver was designed to absorb solar energy from the collector, then transfer the resulting thermal energy to the Stirling engine. Successful testing of receiver/collector assembly yielded valuable inputs for design of the Stirling engine heater head.

Phase I of this program involved solar concentrator renovation and recalibration, while Phase II covered initial receiver design and test, plus engine/alternator development. Although these subassemblies were never tested as a completed system, the engine/alternator combination was successfully tested by the manufacturer.

This experiment ended after completion of engine/alternator tests, but Solar Stirling system development is continuing at JPL on another program with systems in the 15 - 20 kWe class.

FOREWORD

The theoretical advantage in thermal efficiency of the Stirling thermodynamic cycle has been known for many years, but the Stirling cycle has not been widely used in commercial energy conversion applications. One reason is that most Stirling engines are heavy and complicated. These complications make the engines more costly to manufacture than engines employing other thermodynamic cycles and developing equivalent output power. The free-piston Stirling engine is extremely simple, however, as it employs only two moving parts, called the displacer piston and power piston. This simplicity is possible because the output motion is periodic and reciprocal rather than rotary. This characteristic simplicity can be extended to the complete power conversion system by coupling the power piston directly to the plunger of a linear (reciprocating) electrical alternator. The resulting thermal-to-electric power conversion system still has only two moving parts. It is hermetically sealed to prevent loss of the working fluid and the introduction of contamination, and utilizes gas bearings and clearance gap seals. These features allow the engine/alternator to be operated for extended periods without maintenance. Such a combination could find a wide variety of applications ranging from remote underground water pumping to large power generating stations consisting of clusters of separate systems.

The overall objective of the Solar Stirling Experiment was to demonstrate a subscale, integrated, solar-powered electrical power generation module using a free-piston Stirling engine and linear alternator, which was to have been mounted on a parabolic solar collector.

A test-bed collector was needed to obtain practical experience and to determine test receiver performance. For that purpose a 2.9 m (9.5 ft.) diameter parabolic solar collector at the JPL Table Mountain Observatory was refurbished and reactivated. The Table Mountain collector was mounted on a two axis tracker and was ideally suited to the experiment. A cold water calorimeter mounted on the collector and a separate, independently-tracking radiometer were used to measure collector efficiency and solar insolation.

A test receiver was designed, fabricated and tested on the collector. The function of the solar receiver was to absorb the solar energy reflected from the collector and transfer the resulting thermal energy to the Stirling engine. Successful testing of the receiver mounted on the collector yielded critical inputs for the design of the Stirling engine heater head. These tests and some second generation receiver design concepts are described.

Phase I of this program involved the refurbishment and calibration of the solar concentrator, and the design and initial testing of the receiver. Phase II involved subsequent receiver tests and the development of the engine/alternator. Because of funding limitations, the engine/alternator was never tested with the concentrator.

A free-piston Stirling engine using helium as its working fluid was integrated with a linear alternator. The engine/alternator combination was successfully tested at the manufacturer's facility where it produced 930 watts of electrical output power at 30 Hz with 18% engine/alternator efficiency. The engine and alternator designs, and the subsequent testing at Sunpower Inc., Athens, Ohio, and Mechanical Technology Inc. (MTI), Latham, New York, are described.

The 1-kW solar Stirling experiment was discontinued after the tests of the engine/alternator were completed. Solar Stirling system development is continuing on another program at JPL with systems in the 15-20 kWe class.

ACKNOWLEDGEMENTS

The material presented in this report represents a joint effort involving many people. Major contributions were made by the following personnel:

1. F. D. Day, collector system reactivation, and pre-operational testing and calibration of calorimeter and receiver.
2. A. Giandomenico, Task Leader, Phase II
3. P. I. Moynihan, Task Leader, Phase I
4. J. D. Patzold, test facility preparation and test conduction.
5. M. K. Selcuk, thermal systems analysis and system integration
6. Dr. Y. C. Wu, receiver concept and design, and test data analysis.
7. J. W. Anderson, final report editorial assistance.

TABLE OF CONTENTS

	Page
ABSTRACT	iii
FOREWORD	iv
I. INTRODUCTION	1
II. PROGRAM SUMMARY	2
III. CONCLUSIONS	6
IV. RECOMMENDATIONS	6
V. POWER GENERATION CONCEPT	7
VI. COLLECTOR/RECEIVER	9
VII. ENGINE/ALTERNATOR	32
APPENDIX - A 1 kW SOLAR STIRLING ENGINE-ALTERNATOR FINAL TEST REPORT	A-1

LIST OF FIGURES

	Page
2 - 1. Solar Receiver in Operation at the Table Mountain Observatory	3
5 - 1. Stirling Engine/Alternator System	8
6 - 1. Schematic of Calorimeter Test Setup	10
6 - 2. Section View of the Experimental Receiver	13
6 - 3. The Solar Receiver Partially Assembled	14
6 - 4. The Assembled Receiver With Insulation Canister Removed	15
6 - 5. Fully Assembled Receiver With Insulation Canister Installed	16
6 - 6. Receiver Test Flow System	19
6 - 7. Thermocouple Locations on Receiver Heat Exchanger	21
6 - 8. Receiver Cavity Thermocouple Layout	22

LIST OF TABLES

6 - 1. Cold Water Calorimeter Test Results	11
6 - 2. Thermocouple Locations on the Receiver Heat Exchanger Section	23
6 - 3. Summary of Solar Stirling Receiver Test Results	30
6 - 4. Data Points and Description of Conditions	31

I. INTRODUCTION

The U.S. Department of Energy (DOE) Solar Thermal Power Program is aimed at developing advanced solar thermal systems by the mid-1980's that produce electrical energy at a cost which is 25-50% below that based on current technology.

A method of converting solar energy to electrical energy which was proposed to the National Aeronautics and Space Administration (NASA) Office of Energy Programs, consists of a sun-tracking parabolic collector with a thermal energy receiver at the focus coupled directly to a free-piston Stirling engine/ linear electrical alternator. The Jet Propulsion Laboratory (JPL), California Institute of Technology planned to demonstrate a subscale, integrated, solar powered, electrical generation module using a free-piston Stirling engine and linear alternator mounted on a parabolic solar collector.

Because of the simplicity of both the free-piston Stirling engine and the linear alternator, such a combination could be readily applied in situations where low maintenance and high reliability are of prime importance. These same qualities would also be of great advantage in remote locations, since the unit is hermetically sealed and the only input required is solar energy.

The necessary equipment was to be assembled using hardware from previous experiments in combination with an entirely new JPL-designed solar energy receiver and a Stirling engine/linear alternator.

The engine/alternator was procured from Mechanical Technology Inc., Latham, New York. It is an integrated unit capable of being attached to the solar receiver to form a single hermetically sealed system.

Existing JPL hardware consisted of a large parabolic solar concentrator (reflector), a mount to control and support the concentrator, instrumentation, valves, tubing, heaters, etc.

The solar energy receiver was fabricated, and the receiver and collector were tested at the JPL Table Mountain Observatory in May and June of 1977.

The engine/alternator was tested at the manufacturer's facility, but it was not tested as a system with the collector/receiver. The results from the collector and receiver tests, which were accomplished primarily during Phase I, form the larger part of this report, while the final report for the engine alternator development, which was the primary effort during Phase II, is included as Appendix A.

II. PROGRAM SUMMARY

The NASA Energy Systems Division, by means of NASA Task Order RD-169 of NASA 7-100, authorized JPL in 1976 to investigate the feasibility of solar energy conversion with the free-piston Stirling engine/linear electric alternator. In 1977, JPL began testing a solar receiver at the Table Mountain Observatory; Figure 2-1. During this time JPL evaluated proposals to design and build the Stirling cycle free-piston engine and linear (reciprocating) electric alternator.

The overall objective of the Solar Stirling Experiment was to demonstrate a sub-scale, integrated, solar-powered electrical power generation module using a free-piston Stirling engine and linear alternator.

The 2.9m (9.5 ft.) diameter parabolic solar collector mounted on a two-axis tracker at the JPL/Caltech Table Mountain Observatory was refurbished and reactivated to determine the performance of the test receiver, and to obtain the necessary practical experience with solar collectors. A cold water calorimeter mounted on the collector and a separate, independently-tracking radiometer were used to measure collector efficiency and solar insolation.

The function of the solar receiver, which was designed and fabricated to be tested on the collector, was to absorb the solar energy reflected from the collector, and transfer the resulting thermal energy to the Stirling engine. Successful testing of the receiver mounted on the collector yielded critical inputs for the design of the Stirling engine heater head.

The solar test receiver, which was designed and fabricated at JPL, was to function separately from the engine/alternator and provide the following information:

1. Thermal characteristics of the receiver as functions of the working fluid temperature, flow rate, and receiver aperture size.
2. The magnitude of heat losses and heat loss paths.
3. Identification of problems relating to integration of the receiver/collector and engine/alternator.
4. Information for improvements for future receiver designs.

After a procedural and equipment checkout, the JPL solar receiver was tested using solar energy. Efficiencies of about 80% were demonstrated. Operation at 90% efficiency had been projected.

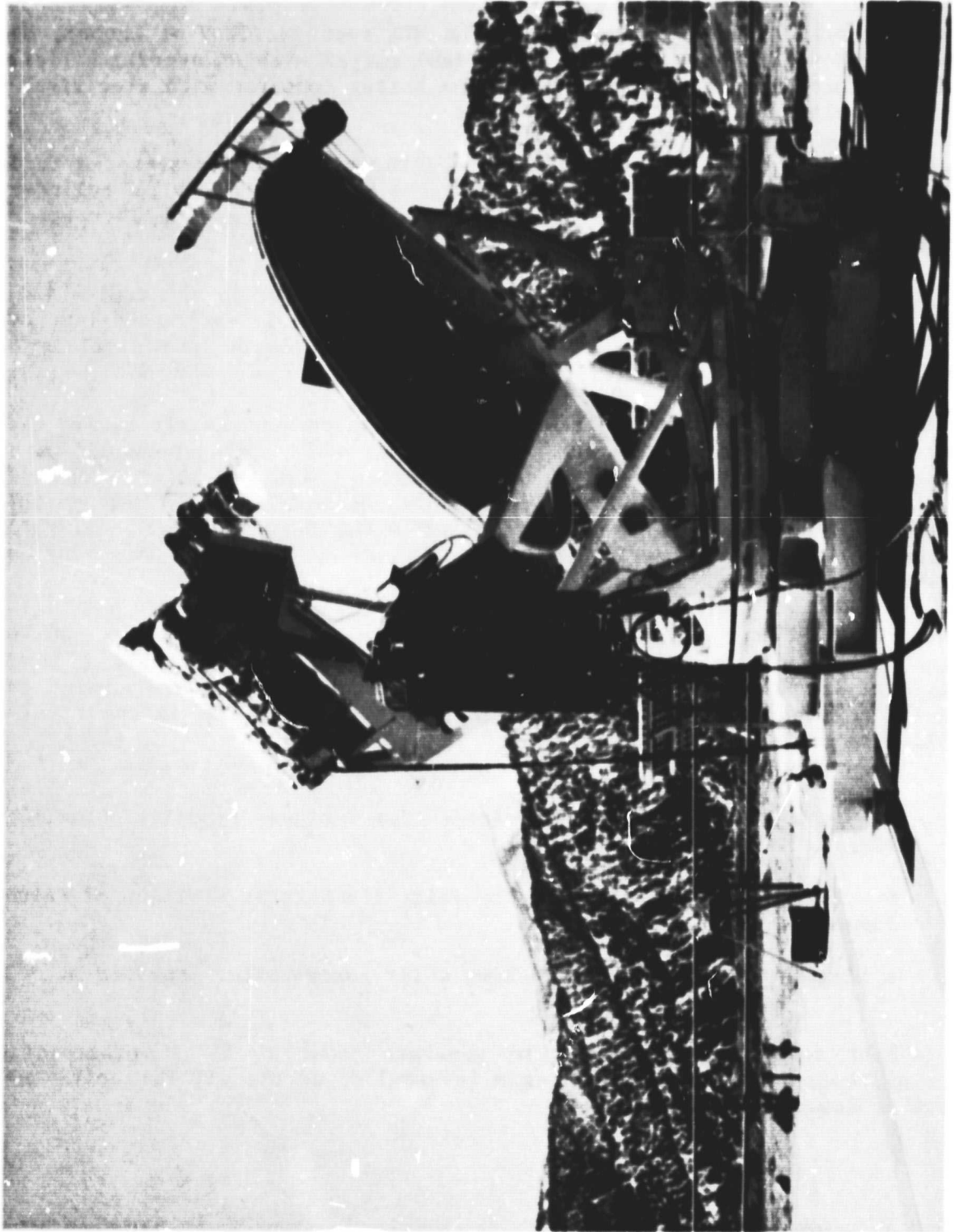


Figure 2-1. Solar Receiver in Operation at the Table Mountain Observatory

ORIGINAL PAGE IS
OF POOR QUALITY

Mechanical Technology Inc. (MTI), Latham, New York was selected to design, fabricate, test, and deliver a prototype free-piston Stirling engine/alternator. Delivery of the engine/alternator in eight months was specified in JPL Contract 954838. The design and test of the engine itself minus the alternator was subcontracted to Sunpower, Inc., Athens, Ohio.

The engine/alternator was tested at the MTI test facility at Latham, New York where it developed 870 watts of electrical output with an overall efficiency of 20%, measured as electrical input to the heater compared with electrical output from the alternator.

Relatively easy starting of the engine/alternator was demonstrated during the acceptance testing by electrically applying heat to the engine cylinder while motoring the alternator using an external power source. Earlier attempts to start the engine by other methods had not proved successful.

During acceptance testing, variation in the heat input to the engine and to the electrical load were made continuously to avoid stalling the engine. Control of the interaction of input heat load and the piston and displacer stroke lengths and phase, as would be necessary in service, was not demonstrated.

All of the tests performed at Sunpower, Inc. on the engine alone, and the tests performed at MTI on the engine/alternator assembly, were conducted using heat input from a resistance-type electrical heater which was built into the engine cylinder head. JPL planned to furnish a replacement cylinder head -- the solar receiver -- which would be interchanged with the electrical heater for the solar experiment, but the replacement cylinder head had not been fabricated at the time the program was terminated.

Through a DOE-NASA Interagency Agreement, the Advanced Research and Development element of the Power Systems Project at JPL is conducting a new effort aimed at demonstrating the feasibility of a much larger solar-powered Stirling engine to produce up to 20 kW of electrical energy. The system involves the following subassemblies:

1. A Stirling engine/alternator combination designed by United Stirling of Sweden.
2. A solar receiver designed by the Fairchild Stratos Division of Fairchild Industries.
3. A 12-meter parabolic sun-tracking solar concentrator provided by JPL.

This test assembly is expected to generate about 20 kW of electricity, and active testing is expected to begin in mid-1981 at the JPL Parabolic Reflector Site at Edwards, California.

The primary effort is to demonstrate the technical feasibility of engine/receiver combinations that are capable of attaining thermal - electric conversion efficiencies of 35-40%. This effort will also provide early testing experience at the system level which will contribute to the design and associated further development of the power conversion package.

This is a new and distinctly separate effort from the one described in this report. However, information and data given in this report could provide a substantial basis for test planning, and for data comparison and evaluation.

III. CONCLUSIONS

The Solar Stirling Experiment produced the first free-piston Stirling cycle engine/alternator and the first JPL solar collector/receiver. The experiment addressed the feasibility of Stirling cycle solar energy conversion as directly as possible, and test data support the conclusion that the concept is viable.

The directly-irradiated receiver operated in thermal equilibrium at more than 70% efficiency, and at temperatures within the limits of ordinary engineering materials. The collector/receiver subsystem operated at 42% efficiency. Bench tests of the free-piston engine/alternator showed that it developed 870 watts of output power at 20% efficiency.

Technical problems with the Stirling engine/alternator were serious and unexpected, but basic technical solutions were demonstrated, albeit at some loss in performance. The goal of a subscale, system-level solar Stirling demonstration was not achieved due to termination of project funding. All basic elements were successfully demonstrated, however, and moderate extrapolation of the free-piston Stirling to higher power ranges appears to be feasible.

IV. RECOMMENDATIONS

The original program concept of a sub-scale system demonstration of solar energy conversion using the free-piston Stirling engine/linear alternator remains sound, but the ultimate verification of the concept has been thrust into the future by the termination of this effort. Serious consideration should be given to further development of 1 kWe hardware for commercial low-power applications, such as marine buoys, radio beacons, etc, where minimum maintenance is desirable.

V. POWER GENERATION CONCEPT

Solar energy conversion by means of a free-piston Stirling engine and linear electric alternator is of special interest because of the simplicity of the engine/alternator itself and its potentially high overall energy conversion efficiency.

High efficiency is attributable to the fact that the Stirling thermodynamic cycle accepts and rejects heat at constant temperatures, and therefore can potentially approach the ideal performance of the Carnot thermodynamic cycle more closely than any other heat engine. The special significance of high efficiency in solar thermal energy conversion is that the system cost is very strongly driven by the cost of the solar collector, and for a given electrical output, the area of the solar collector can be reduced as the heat engine efficiency is increased.

The conversion of solar energy to electrical energy by means of the free-piston Stirling engine/linear alternator requires four steps: (1) the capture and concentration of solar energy by the collector; (2) the conversion of solar to thermal energy in the receiver; (3) the conversion of thermal to mechanical energy in the Stirling engine; and (4) the conversion of mechanical to electrical energy in the alternator. Figure 5.1 identifies the major parts of the engine/alternator.

The solar energy collector, a large parabolic reflector supported in a two axis collector mount, concentrates several kilowatts of solar flux. The collector mount follows the sun's motion across the sky, holding the concentrated solar flux in the cavity of the solar receiver.

The solar receiver, operating at internal temperatures as high as the materials of construction will allow (in order to achieve the highest possible engine efficiency), converts the solar energy to thermal energy. The thermal energy is transferred into the helium gas working fluid of the receiver and Stirling engine. The helium gas circulates between the solar receiver and the cylinder head.

The free-piston Stirling engine expands the heated helium gas, converting the heat energy to kinetic, or mechanical energy, on the reciprocating power piston. The motion of the piston is harmonic, and is controlled in frequency by the physical constraints of the helium gas and the mass of the moving pistons.

The linear (reciprocating) alternator converts the mechanical energy in the moving power piston to electrical energy. The piston itself is configured to form the pole piece in the magnetic field of the alternator. The magnetic field is switched by the moving pole piece so that an electrical current is induced in the output winding of the alternator.

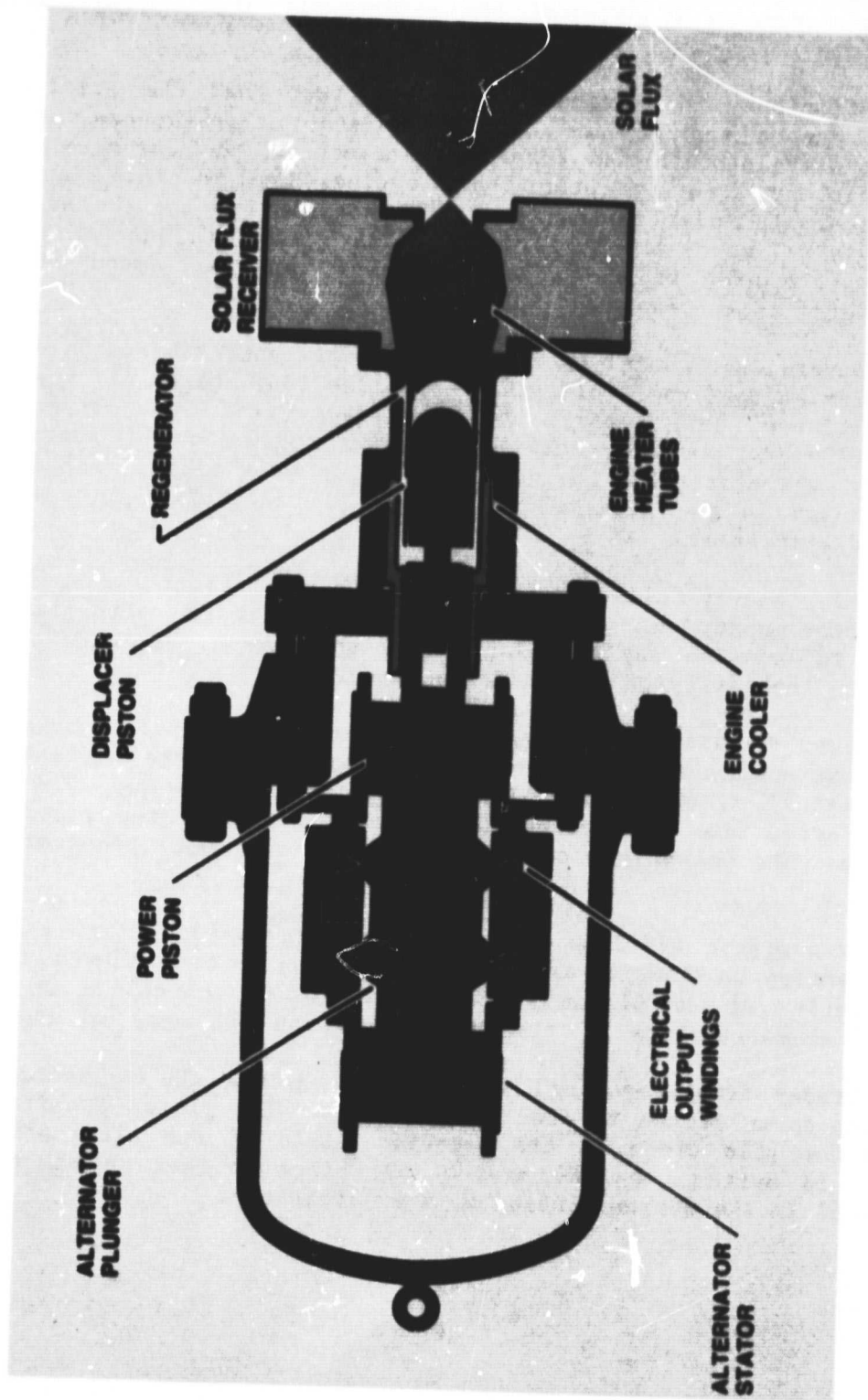


Figure 5-1. Stirling Engine/Alternator System

VI. COLLECTOR/RECEIVER

The work reported in this section was accomplished during Phase I of this program.

The Collector

The solar collector (See Figure 2-1) is a vapor-deposited nickel paraboloidal mirror 2.90 m (9.5 ft.) in diameter with a 1.76 m (5.76 ft.) focal length and 45° rim angle. It has a theoretical focal size of 1.59 cm (5/8 in), and thus has a very high concentration ratio. The collector had been used in a number of previous applications including the operation of a thermionic device and vaporization of moon rocks.

The collector and its support systems were refurbished for this program. A room temperature calorimeter test was conducted to quantify collector performance. The calorimeter arrangement and a summary of the calorimeter test results are depicted in Figure 6-1 and in Table 6-1, respectively. The collector efficiency, (defined as the ratio of the energy collected to the total energy impinging on the mirror), was 60% in the "as-found" condition and 66% in the cleaned condition.

The receiver was aligned with the collector using the light of a full moon. The size and shape of the focal point was determined during this alignment. Briefly, the smallest focal size was found to be 2.03 cm (13/16 in) compared with the theoretical 1.59 cm (5/8 in). The focal shape was seen to be elliptical when displaced along the mirror axis, and this information was used in the final alignment of the receiver.

The Receiver

The function of the solar receiver is to capture the solar energy reflected from the collector and to efficiently transfer the resulting thermal energy to the Stirling engine. Thus, the receiver must meet the operational requirements of both the collector and the engine.

For a Stirling engine to operate at high efficiency, it is necessary to maintain the highest temperature at the heat source, to minimize the heater head volume, and to minimize the pressure drop in the working fluid during its passage through the receiver. For maximum receiver efficiency, it is desirable to minimize both surface temperature and aperture size (the opening through which the solar energy passes). These conflicting requirements impose constraints on the receiver design. A lack of specific engine thermal and mechanical information as well as an incomplete understanding of the collector solar flux distribution added to uncertainties in the early stages of the receiver design process. It was therefore decided to accomplish the receiver design task in two separate steps. The first step was to design an experimental receiver based on available information and readily available materials, while the final receiver would be

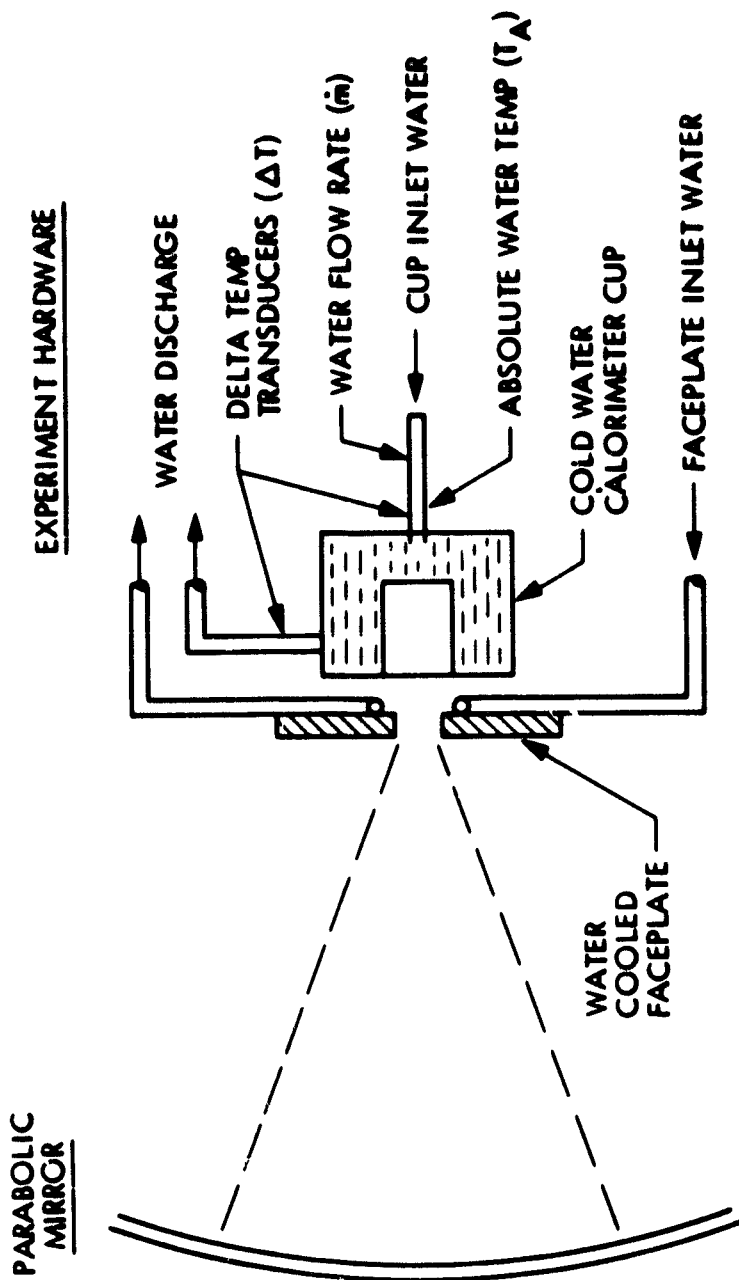


FIGURE 6-1. Schematic of Calorimeter Test Setup

Table 6-1 - Cold Water Calorimeter Test Results

Date	Time	m (lbm/sec)	Ia (°F)	I (°F)	r (mm/cm)	P Incident	P usable	η (%)	Comments	
9/21/76	0817	0.147	65.0	13.0	87.0	5.73KW	2.00KW	34.9	Initial alignment	
	0825	0.148	67.0	19.0	86.5	5.83	2.92	50.8	Realignment 1	
	0852	0.146	64.75	21.5	93.0	6.12	3.31	54.0	Realignment 2	
	0907	0.146	64.5	23.75	94.0	6.19	3.67	59.2	Realignment 3	
	0925	0.147	64.8	24.25	96.0	6.32	3.76	59.4	Realignment 4	
	0947	0.148	65.8	24.6	97.0	6.39	3.84	60.1	Adm. completed	
	1000	0.148	65.0	24.75	97.0	6.39	3.86	60.4	Peak	
	1015	0.149	65.0	23.9	96.0	6.32	3.74	59.2	Transient	
						<u>Cleaned Mirror</u>				
	9/21/76	1623	0.147	64.6	20.0	75.0	4.94	3.10	62.7	Some tracking error
9/22/76	1629	0.147	65.0	20.0	71.5	4.71	3.10	65.8	Steady-state	
	0730	0.142	57.0	18.2	67.5	4.45	2.72	61.3	Transient Peak	
	0739	0.145	64.5	19.4	72.0	4.74	2.96	62.5	Transient Peak	
	0751	0.146	66.5	16.7	63.0	4.15	2.57	62.0	Transient Notch	
	0820	0.145	64.0	23.45	84.0	5.53	3.58	64.8	1.5 min. Peak	
	0936	0.145	64.3	24.9	90.5	5.96	3.80	63.8	Transient Peak	
	0951	0.145	64.5	27.6	97.0	6.39	4.21	66.0	Steady State	
	0955	0.145	64.6	27.9	97.5	6.42	4.26	66.4	Steady State	
	0956	0.145	64.6	26.5	93.8	6.18	4.06	65.7	Small Notch	
	1010	0.145	64.6	27.9	98.7	6.50	4.27	65.7	Steady State	
1045	0.145	64.8	28.6	100.0	6.59	4.36	66.2	Steady State		
Max Solar Flux on 9/21/76			97.5 mm/cm ²						r = Radiometer output	
			100.0 mm/cm ²						P = Power	
									η = Efficiency	
									m = Water Flow rate	
									Ta = Absolute Temperature	
									T = Water Temperature Diff.	

designed to match engine performance. However, the second design was never undertaken because of the difficulties encountered later in fabrication and test of the engine/alternator.

The primary receiver design considerations were thermal efficiency and the ability to generate test data for future use.

To satisfy the requirements of the collector, the receiver was required to be capable of absorbing 5.0 kW(t) of thermal energy at the highest insolation condition, and 4.0 kW(t) under nominal conditions.

The engine operating conditions required that the engine operate with gaseous helium at a nominal temperature of about 650°C (1200°F) within a pressure range of 600 to 1200 psia, at an operating frequency of 30 to 60 Hz. To estimate the helium flowrate, the engine heater head internal diameter was assumed to be 5.72 cm (2.25 in), and the displacer stroke was assumed to be 4.00 cm (1.575 in) based on proposed engine configuration. The volume of the receiver was constrained to be no more than 32.18 cm³ (1.964 in.³). It was estimated that a nominal flowrate through the receiver would result in a receiver cavity temperature on the order of 813°C (1500°F) to 871°C (1600°F) with the potential of higher temperature hot spots.

It was decided to use Inconel 718 for the heat exchanger tubes, and to conduct the receiver tests within its safe limit. The final configuration was to have been fabricated from Inconel 617 because of its superior properties, but the project was terminated before that change could be incorporated.

Several concepts were examined for the heat exchanger section of the receiver, including simple tubes (either directly irradiated by the solar flux or imbedded in refractory or storage materials), a grooved heater head, a porous heater head, a quartz window, and a tube-in-shell design (NaK in the shell and the engine working fluid in the tubes). Many concepts were rejected because of excessive design complexity. The concept of the heat exchanger tubes directly irradiated by the solar flux was selected because of its simplicity, potentially easy repair, and its capability of being modified later with a thermal storage feature. Figure 6-2 shows a section view of the receiver, and Figures 6-3 through 6-5 show the receiver test hardware.

The complete receiver is composed of four primary parts: (1) a heat exchanger section consisting of 34 pairs of Inconel 718 heat exchanger tubes brazed to an Inconel 718 head plate, (2) a contoured ceramic receiver body, (3) an aperture piece to provide variable aperture sizes, and (4) a stainless steel canister filled with calcium silicate to minimize conduction heat loss. The receiver was designed to be incorporated into the Stirling engine cylinder head as an integral part.

The 34 pairs of Inconel 718 tubes were 0.318 cm (1/8 in) O.D. with 0.041 cm (0.016 in) wall thickness. Each pair of tubes was 8.38 cm (3.30 in) long on both the inlet and outlet sides (total length, 16.76 cm), and were bent at the middle with the ends brazed to the inlet and outlet manifolds of the head plate.

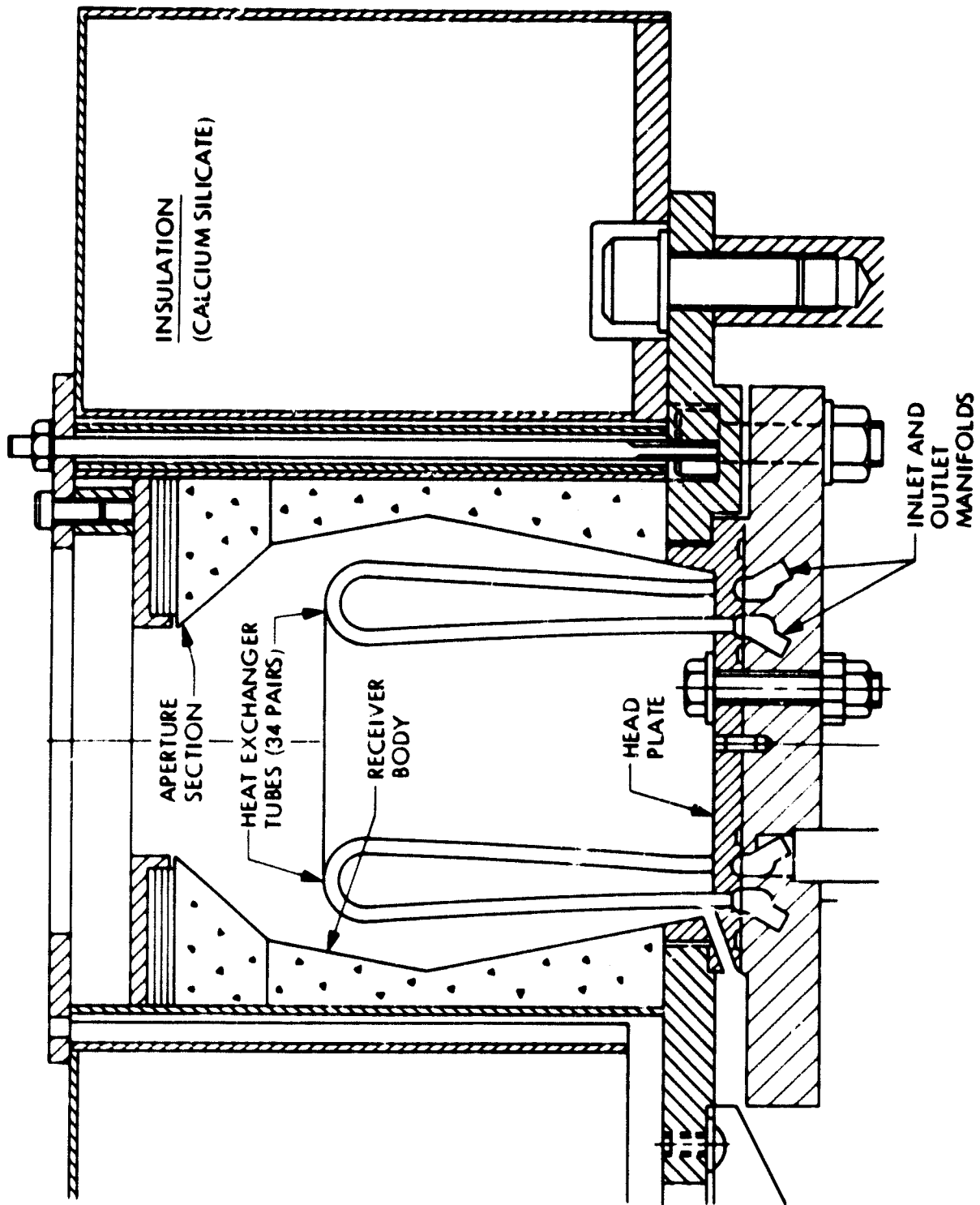


FIGURE 6-2. Section View of the Experimental Receiver

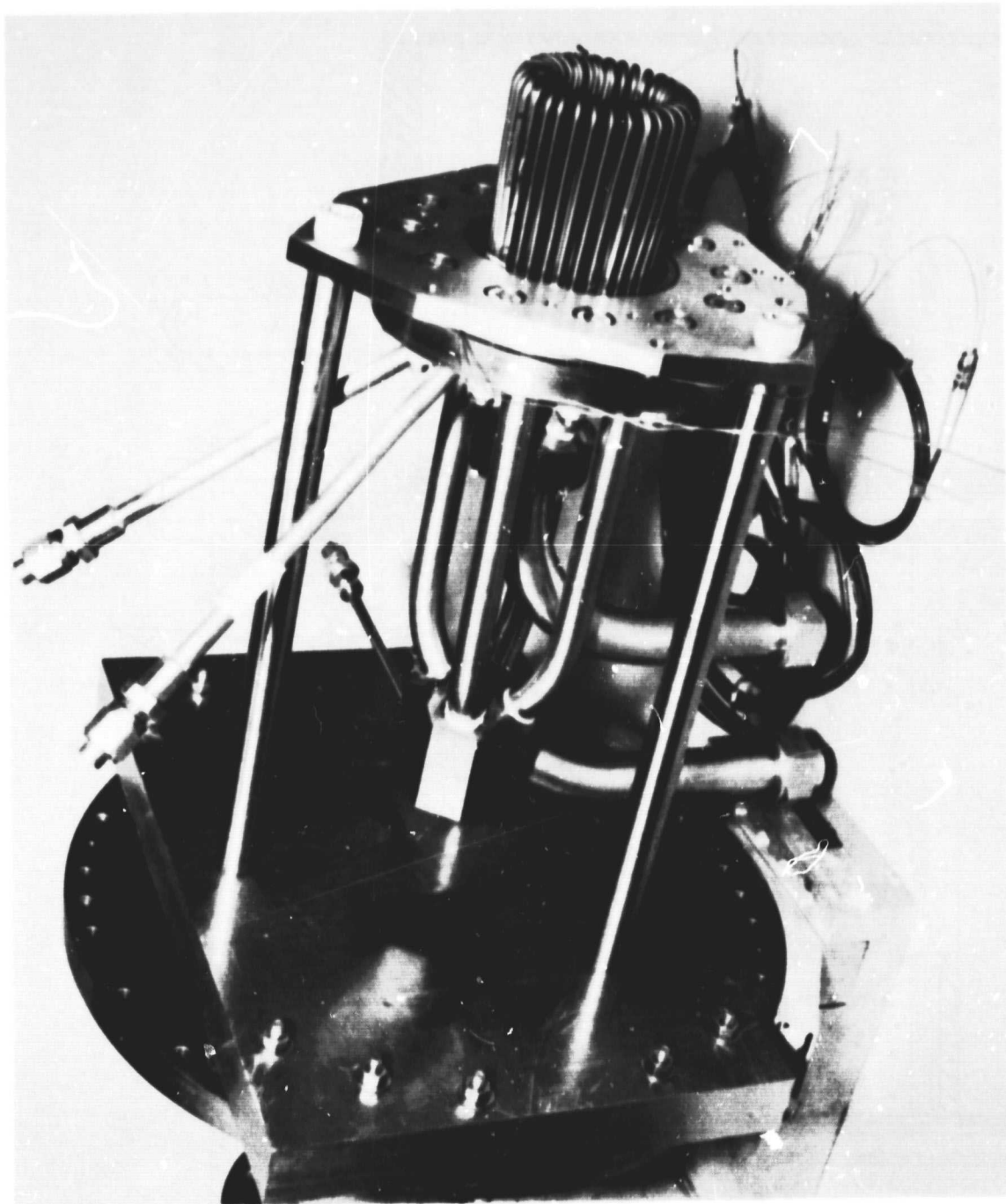


Figure 6-3. Solar Receiver Partially Assembled

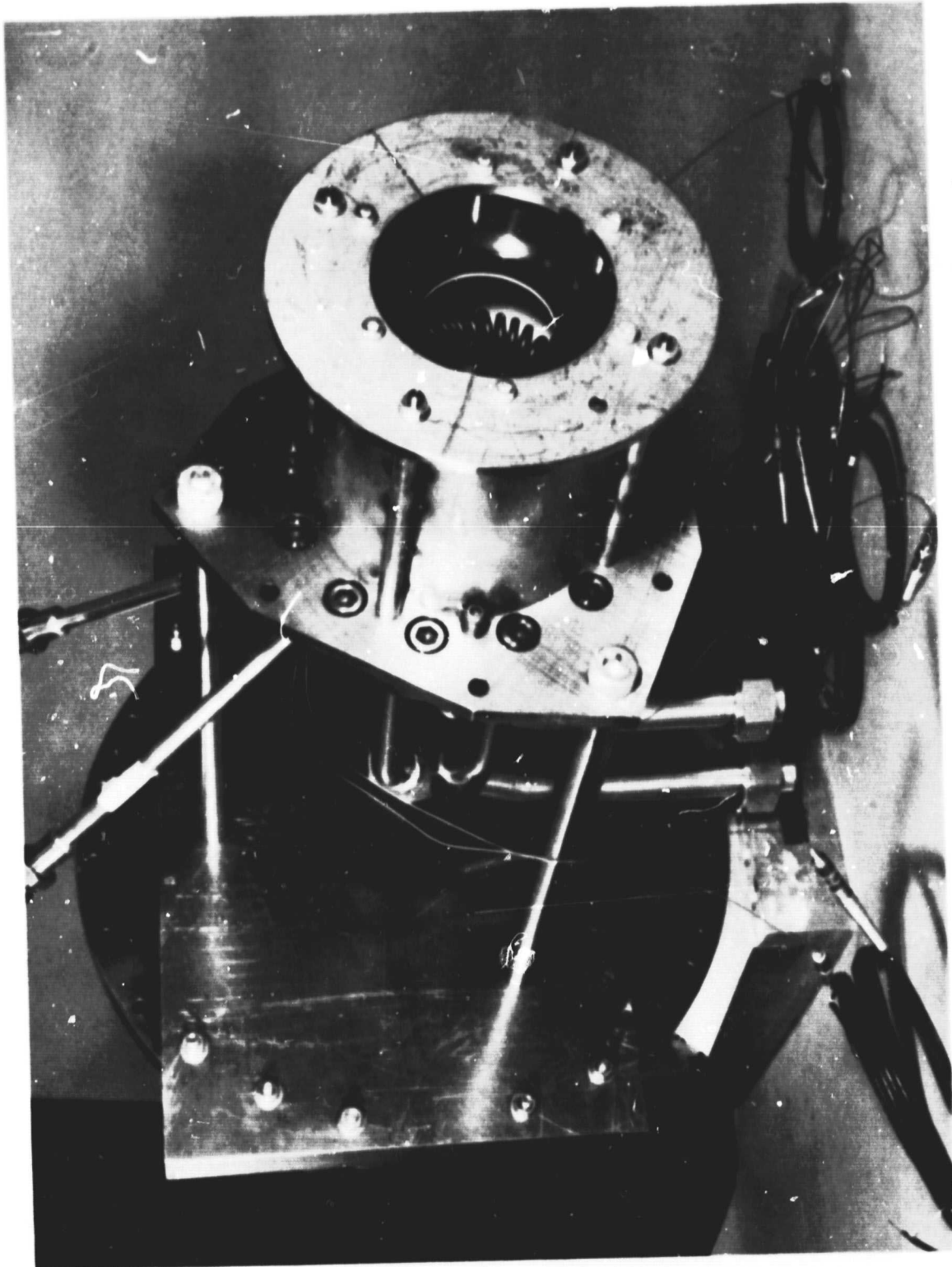


Figure 6-4. The Assembled Receiver with Insulation Canister Removed

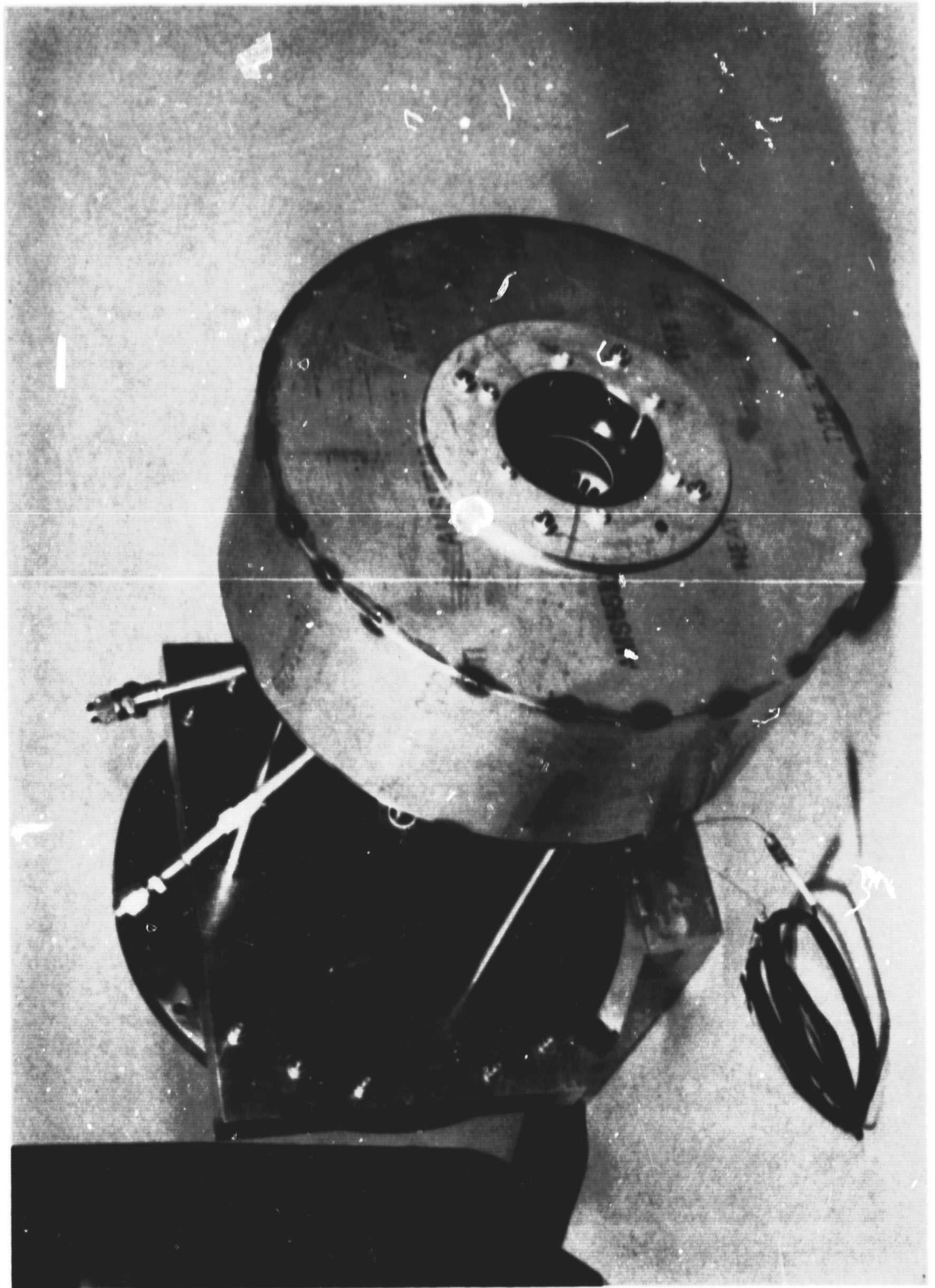


Figure 6-5. Fully Assembled Receiver with Insulation Canister Installed

Solar flux from the central half of the collector would impinge on the inner side of the receiver tubes (toward the center of the cavity). The flux from the outer half of the collector would impinge on the inner wall of the receiver cavity and then be reflected to the tube side facing the wall. This arrangement was expected to reduce the maximum flux density on the tubes and to provide an even distribution of the heat flux.

Receiver Fabrication

No problems were encountered in the fabrication of the receiver, but heat exchanger tube and receiver body ceramic materials were difficult to obtain, and created some difficulty in meeting the program schedule.

Inconel X-750 was initially selected for the heat exchanger tubes, but was not available from local suppliers. For a time, stainless steel was considered with the intent of testing the receiver at a lower-than-desired temperature to maintain the required strength. However, Inconel 718 was selected as an acceptable substitute for the final receiver design.

The ceramic receiver body proved to be the most difficult receiver part to fabricate. The initial castings were too porous and the surfaces were rough. Thermo-sil Castable 120 from Thermo Material Corporation was found to yield a very smooth and reflective surface, a fairly solid body, and very low thermal conductivity. An attempt was made to find a glazing material that would improve the ceramic reflectivity, but all the glazed surfaces showed a slightly lower reflectivity than the non-glazed ones. It was therefore decided to use the bare ceramic surface.

Test Configuration

The overall receiver test configuration consisted of the solar collector, the working gas test loop, and the data acquisition system.

Testing was planned at flowrates which yielded Reynolds numbers with the same heat transfer coefficient as the engine in solar operation. For a Stirling engine with helium at 40 atmospheres (588 psia), 650°C (1200°F), and a frequency of 30 Hz, the equivalent helium flowrate was calculated at 103 lbm/hr. For helium operating at the test conditions of 20 atmospheres (300 psia), and 650°C (1200°F), the equivalent flowrate is 110 lbm/hr; operating at these same conditions, the equivalent nitrogen flowrate was 664 lbm/hr.

The Test Loop

The working fluid in the Stirling engine flows first in one direction and then in the other through the heater head. An ideal test loop would simulate an oscillatory flow, but such a flow simulation was deemed too complex to be undertaken within the scope of this program. A closed loop, continuous flow system that included a circulation compressor was considered, but abandoned in favor of a simpler, open loop, continuous flow system.

No circulation compressor was required for the open loop system because the gas was vented into the atmosphere after use. Instead, a pressurized gas supply of 1274 standard m³ (45,000 SCF) at 150 atmospheres (2,200 psig) was used. Because of the higher cost of helium gas, nitrogen gas was used for the procedural checkouts and for all flow conditions in which helium was not required.

Figure 6-6 is a schematic diagram showing the details of the flow system, which includes the flowmeter, the pressure control system, and the heat exchanger and heater. Both the helium and the nitrogen supplies are shown.

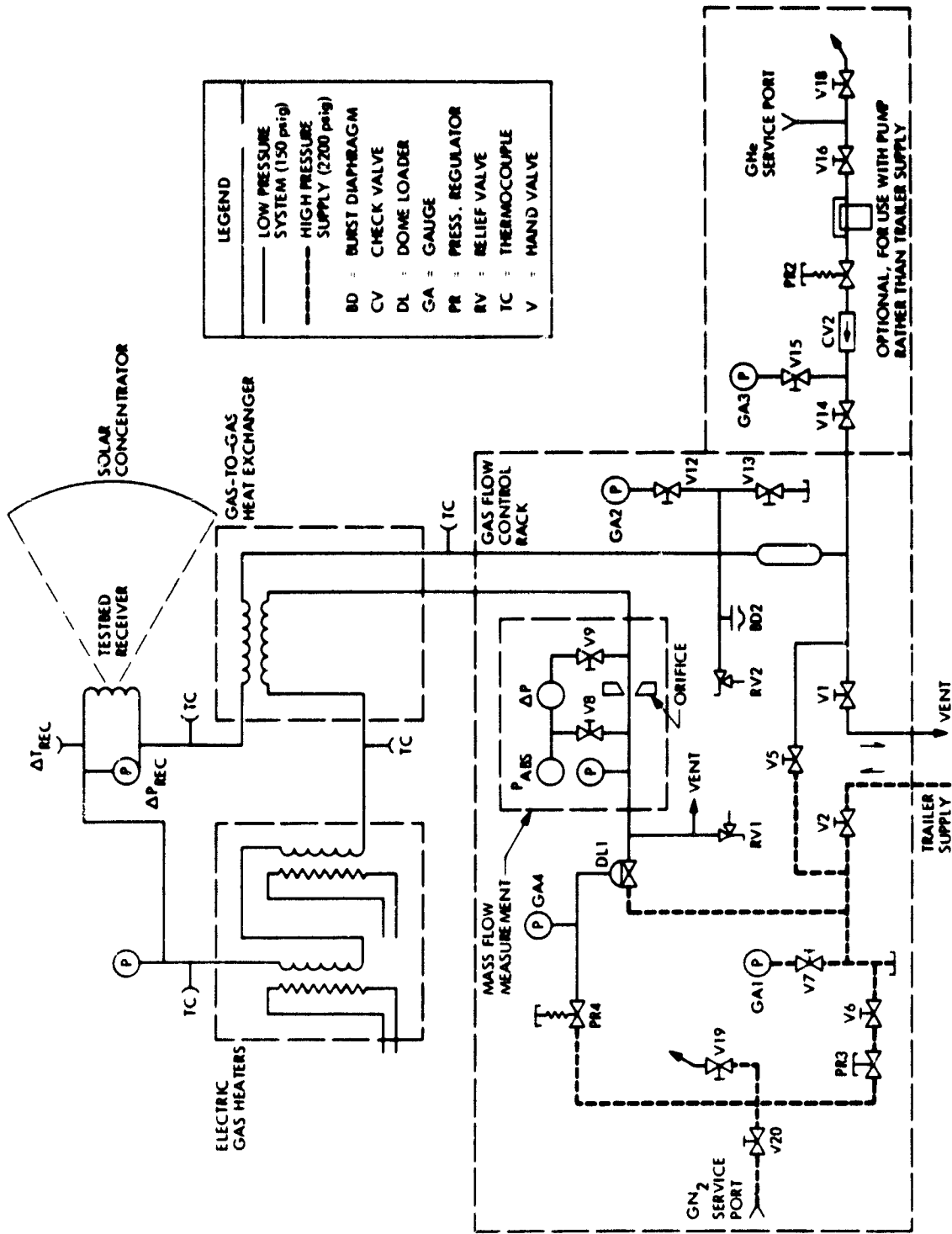


FIGURE 6-6. Receiver Test Flow System

Receiver Instrumentation

Instrumentation of the receiver was difficult because of the anticipated high cavity temperatures. A long portion of the thermocouple leads on the heat exchanger tubes was, by necessity, exposed to high solar flux. Various approaches, including the installation of the thermocouples on the inside of the tubes, were examined. The temperature was measured from outside of the tube with chromel-alumel thermocouples with 0.081 cm (0.032 in) O.D. sheaths. The thermocouple beads were resistance welded to the tubes and covered with 0.025 cm (0.010 in) thick, noncontacting stainless steel radiation shields. A total of nine thermocouples (T3, T4, T5, T6, T8, T9, T10, T11, and T12) were installed on the heat exchanger tubes and one (T18) on the head plate, as shown in Figure 6-7 and Table 6.2.

The thermocouples on the ceramic cavity wall were located about 0.025 cm (0.101 in) from the surface of the inner cavity wall. This required the drilling of 0.159 cm (1/16 in) diameter holes from the outer side. Six thermocouples, four of which (T14, T15, T16, and T17) were installed near the inner surface and two (T19 and T20) near the outer surface, were provided for the cavity wall, as shown in Figure 6-8.

In addition, one thermocouple (T13) was located on the aperture plate, and two differential thermocouples (T21, T22) were provided for the measurement of the temperature difference across the outer insulation layer.

One immersed thermocouple (T29) was provided for the measurement of the receiver inlet working fluid temperature. An immersion thermocouple was also installed at the gas outlet and connected to the inlet to form a differential for determining the temperature difference between the inlet and outlet gas.

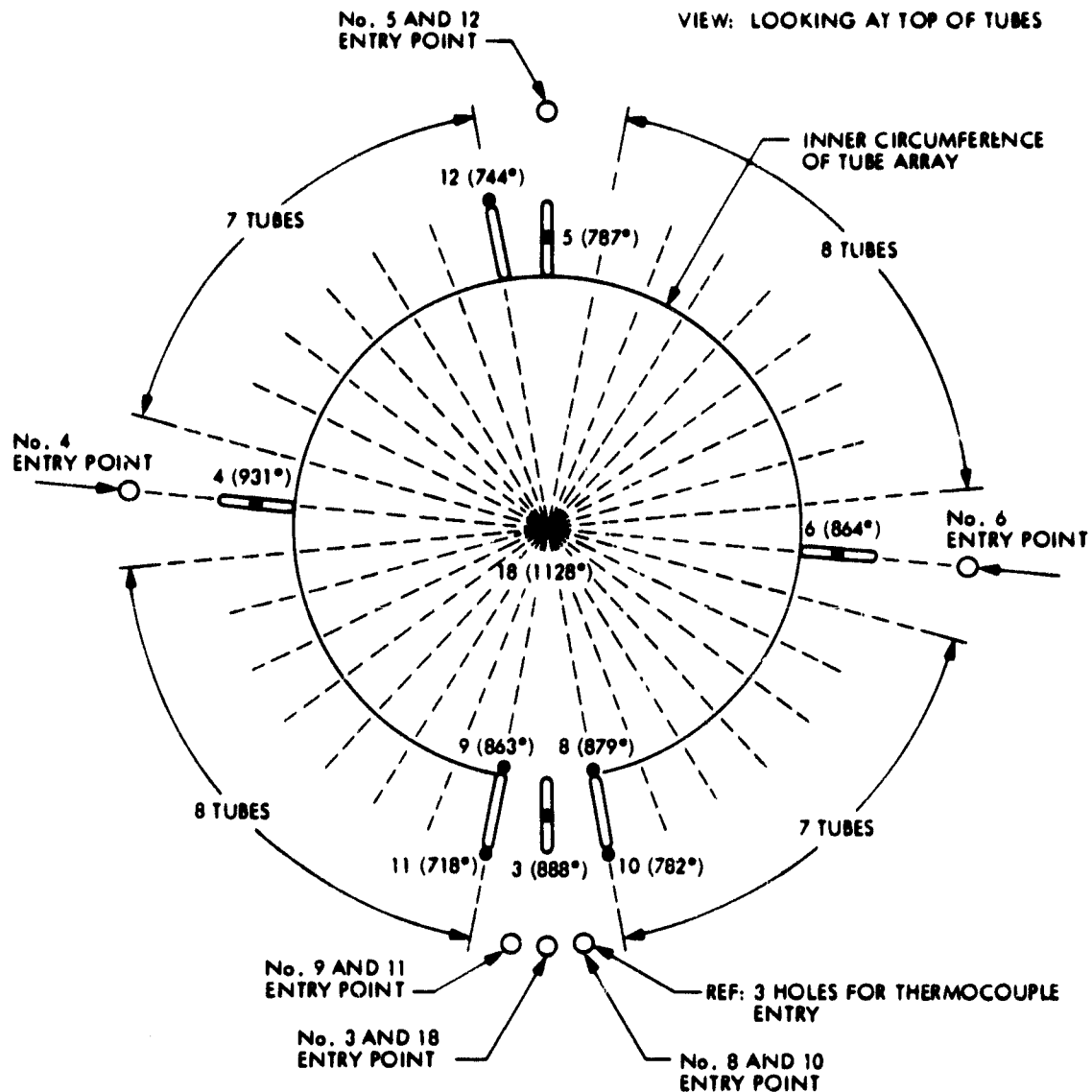
Two pressure measurements were made at the receiver to determine the absolute pressure of the gas entering the receiver and the pressure difference between inlet and outlet gas.

To determine flowrate and heater temperature at the helium inlet, pressure and temperature measurements were also provided at several other locations in the flow loop, as shown in Figure 6-8.

A shutter was installed at the receiver aperture as an emergency means of terminating the solar flux.

Data Acquisition System

The data acquisition system consisted of strip chart recorders and a paper tape printer. The more important readings which required continuous monitoring, such as the radiometer, the working fluid inlet-outlet temperature differential, the aperture plate temperature, one heat exchanger tube temperature, the gas supply temperature, and the pressure differential across the flowmeter, were continuously displayed on the strip chart recorders and were therefore available



NOTE: NUMBER IN PARENTHESIS NEXT TO THERMOCOUPLE NUMBER IS TYPICAL OPERATING TEMPERATURE IN °F

FIGURE 6-7. Thermocouple Locations on Receiver Heat Exchanger

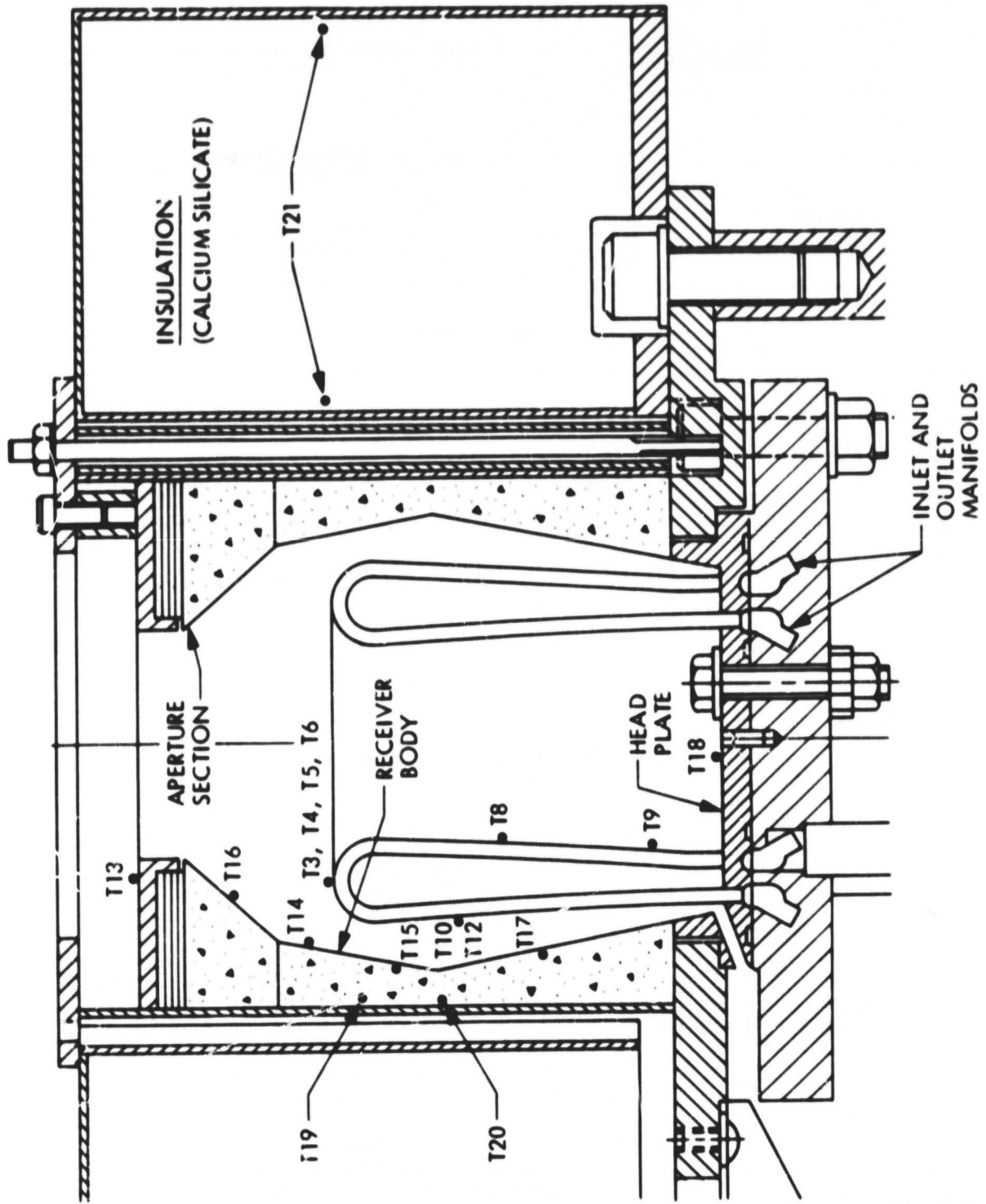


FIGURE 6-8. Receiver Cavity Thermocouple Layout

TC	LOCATION	WELD PRESS		DISTANCE: MEASURING JCT TO SHIELD. (APPROX.)
3	Top (inside .060")	1.5	4, 6, 8 W/B	.050"
4	Top	"	4, 6, 8 W/B	.060"
5	Top	"	4, 6, 8 W/B	
6	Top	"	4, 6, 8 W/b	.060"
8	Inside, 2.03" from Base	"	2, 3, 4 W/S	.030"
9	Inside, .650" from Base	"	2, 3, W/S	.045
10	Outside, 2.03" from Base	"	2, 3, 4, 5 W/S	.065"
11	Outside, .650 from Base	"	2, 3, 4 W/S	.045"
12	Outside, 2.03" from Base	"	2, 3 4, 5 W/S	.060"
13	Center, .115" from Hole	"	1.5 W/S Only	.050"

Table 6-2 Thermocouple Locations on the Receiver Heat Exchanger Section

for real-time corrective action, if necessary. All the other data were recorded in digital form on paper tape. The printout rate for this recorder was one channel per second.

Test Plan and Test Procedures

Since one of the concerns during the test was the possible burn-out of the receiver heat exchanger tubes, the test was structured so that the important data would be acquired before burn-out could occur. This dictated a test plan with the following test sequence:

1. Install the 2" diameter aperture prior to the test.
2. Start the test with the nominal gas flowrate entering the receiver at room temperature.
3. Increase the inlet temperature in steps from room temperature to 316°C (600°F), 427°C (800°F), 538°C (1000°F), and finally 650°C (1200°F) during subsequent test runs.
4. Repeat the above tests at flowrates of 75% and 50% of the nominal values.
5. Test aperture sizes of 3.81 cm (1.5 in) and 2.54 cm (1.0 in) diameter if the results of the test runs above indicate that the quantity of reradiated energy would be reduced.

Receiver Tests

The first receiver test was conducted in the late afternoon of May 19, 1977 and the test duration was 2.5 minutes. The purpose of the test was system and procedural checkout. The working fluid was nitrogen, and receiver aperture size was 5.08 cm (2.0 in). After the test, oil from the fabrication process was observed on some of the receiver heat exchanger tubes and is thought to have been the cause of smoke observed during the test. Post-test inspection revealed that the Inconel aperture plate had developed two discolored spots. The discoloration was due to excessive heating, and was an indication of receiver misalignment which resulted in the impingement of a portion of the solar flux on the aperture plate.

The second test, of 42 minutes duration, was conducted on May 20, 1977. Some useful receiver performance data were obtained. Early in the test, smoke from the residual oil continued to come from the receiver cavity. Later in the test the insulation on the inlet fluid heater also started to smoke. Due to over-heating from the solar collector, the aperture plate reached a temperature of 1205°C (2200°F), and had become completely discolored.

The highest indicated helium inlet and outlet temperature differential recorded at full flowrate was slightly less than 33°C (60°F). This implied an energy collection on the order of 2 kW, which is far below the expected value of nearly 4 kW. As a result, the methods of determining the flowrate and the receiver differential temperature were investigated. The calculated flowrate may have been less than the actual flowrate because the differential pressure transducer used in the calculation of flowrate performed erratically during the test.

A second error was discovered in the method of measuring the differential temperature across the receiver. The hot side junction of the differential thermocouple was located in the shadow of the receiver and its support arm, which resulted in a much lower outlet temperature measurement and a misleadingly low calculated energy collection rate.

Because of these findings, the results obtained in this test were not considered representative of the receiver performance. Further testing was postponed until the following instrumentation changes were made:

1. The flowmetering section was checked and the differential pressure transducer was replaced.
2. Surface temperature thermocouples were tack welded onto the inlet and outlet lines of the receiver and were covered by approximately two inches of insulation.
3. The receiver was realigned.

The third and final test was conducted in the late morning of June 1, 1977 and its duration was three hours and 20 minutes. One obvious change in these test data compared with earlier data was the drop in the aperture plate temperature from 1205°C (2200°F) to 760°C (1400°F), which indicates better receiver alignment. Because the electrical heaters were becoming quite heavily eroded from extensive operation at high temperature, the gas inlet temperature was constrained to 1000°F maximum. The resulting data were less extensive but were considered acceptable and representative of receiver performance. The test results are summarized in Table 6-3, and generally indicate performance efficiencies of up to 87%. Periods of operation above 90% efficiency had been expected.

Receiver Performance

This section presents the theoretical basis for determining the performance of the solar receiver. The equations used in calculation of the performance from the experimental data are summarized and a brief discussion of range of validity and expected accuracy is given.

The Overall Receiver Heat Balance

The overall heat balance of the receiver can be closely approximated by the equation,

$$Q_r - A_t h_t (T_t - T_f) - A_a \epsilon_a \sigma T_{a_{eff}}^4 - \sum A_i \epsilon_i \sigma T_i^4 - \sum G_j (T_{a_{eff}} - T_o) - \sum A_k h_k (T_k - T_o) = 0$$

where

- Q_r = solar radiation energy entering the receiver cavity
- A = effective heat transfer area
- h = effective heat transfer coefficient
- T = temperature
- ϵ = effective emissivity
- σ = Stefan - Boltzmann constant, 5.67×10^{-12} watts/cm² - K⁴
- G = effective thermal conductance

with subscripts

- t = heat exchanger tubes
- f = working fluid
- a = aperture
- eff = effective
- o = ambient

The first term represents the total solar energy available for collection.

The second term, $A_t h_t (T_t - T_f) = \dot{W} C_p \Delta T$, where \dot{W} is the working fluid flow-rate, C_p is the specific heat, and ΔT is the change in the working fluid temperature, represents the energy carried away by the working fluid.

The third term represents solar energy reradiated from the receiver aperture unconverted from solar to thermal energy.

The other three terms represent losses by radiation, conduction, and convection after the solar-to-thermal conversion. For a well-designed receiver, these terms should be small compared with the first three. By the proper fitting of the test data, the equation can be used in various ways for the evaluation of any one of the parameters, as will be seen below.

Receiver Efficiency

The receiver efficiency, η_R , is defined as the ratio of the collected energy to the total energy entering the receiver cavity, or

$$\eta_R = \frac{A_t h_t (T_t - T_f)}{Q} = \frac{\dot{m} C_p \Delta T}{Q}$$

$$= 1 - \frac{\sum \text{losses}}{Q}$$

The second expression was used in calculating receiver efficiency for data reduction, and the first and second expressions were used to evaluate the effective heat transfer coefficient of the heat exchanger tubes, h_t . In principle, the third expression can be used to check the result from the second. Unfortunately, the instrumentation was not sufficient to accomplish this task.

Cavity Wall Temperature

A portion of the cavity wall in the receiver was shaped to reflect the solar flux fluid onto the lower part of the heat exchanger tubes, thereby providing a more uniform distribution. Therefore, a highly reflective cavity wall was desired. The unglazed ceramic surface exhibited an average solar absorptivity of 0.156 and was deemed acceptable.

A simplified analysis of the illuminated portion of the ceramic surface considering only the effects of its solar absorptivity α_{w1} and its IR emissivity ϵ_{w1} can be made, neglecting the conductive effects. The heat balance equations for the illuminated surface, designated by the subscript w1, can be written as

$$Q_{w1} = \sum_k f_k \sigma (T_{w1}^4 - T_k^4) = q_{w1} \alpha_{w1}$$

where Q_{wi} is the total incident solar energy on the illuminated portion of the ceramic wall, q_{wi} is the flux density, and f_k is the view factor between the illuminated surface and any other surfaces with subscript k at temperature T_k . Because of the difficulty in the rigorous evaluation of f_k , this equation is useful for quick assessments only.

Absorption Energy Losses

Energy losses are caused by absorption and misalignment, and by the shadow cast on the mirror by the receiver and its support structure. Absorption and misalignment losses were present during both the low temperature calorimeter test and the receiver test, but the difference between the two was deemed small and extremely difficult to quantify.

However, the shadow cast on the mirror was of considerably greater magnitude during the receiver test, because of the larger area shadowed by the receiver, its support arm, and the insulation around the electrical heaters. The magnitude of this difference was assessed as being about 6.1% from photographs taken during the two tests where the shadow covered 8.4% of the total mirror surface during the receiver test and only 2.3% during the calorimeter test.

Receiver Energy Losses

The heat losses of the receiver are by radiation, conduction, and convection, and are represented by the last three terms in the receiver heat balance equation. For a well-designed, well-insulated receiver the radiation heat loss through the aperture will be the dominant loss. The heat losses by conduction and convection should be less significant.

Receiver Test Results

The first test consisted of a procedural and equipment check-out which was not intended to produce data. Serious instrumentation difficulties were experienced during the second test so that the data collected were not useful. The results of the third test are representative of the receiver performance and are presented herein as an overview, with important test events summarized in Table 6-3. Each event is identified by an I.D. number which is a time indicator corresponding to the number of paper tape printouts from the start of the test. The elapsed time from the start of the test is also shown in minutes for each event.

Table 6-4 shows all the test data selected for analysis with pertinent comments for each test. The selection of test data was based on inlet gas temperature, and some of the test data represent transient states, such as changes in solar intensity during cloud passage. The interpretation of these specific data is difficult and less meaningful than the interpretation of steady state data. For example, test data with I.D. 199 and 377 show receiver efficiencies of more than 100%. It can be seen in Table 6-4 that the solar intensity was changing rapidly during these two tests. Since the response of the radiometer is very rapid and

the system has very high thermal inertia, the solar intensity used in the efficiency calculation does not correspond to the temperatures and flowrate. Therefore, the efficiency calculated for these specific cases is not valid.

For the calculation of the receiver efficiency, two collector efficiencies were used. The 60% number is representative of the collector efficiency found after several years of non-use; the 66% efficiency represents the collector efficiency immediately after the mirror was cleaned. Since the receiver tests occurred several months after the mirror was cleaned, the actual mirror condition at the time of receiver tests should be somewhere between these two conditions. Thus, the two calculated efficiencies may be considered as the high and low limits of receiver efficiency.

The large differences in efficiencies for the data points displayed are attributed to transient effects. Some of the data were taken while the inlet electrical heater was actuated. Since the heater power input is greater than the solar power input, the inlet gas temperature can "overtake" the exit gas temperature and result in erroneous apparent efficiencies. Efficiencies above 70%, however, were established for steady state performance.

Because only two flowrates were tested and the fluid temperature range was relatively narrow, extensive correlation of the receiver efficiency, flowrate, and gas temperatures cannot be established from these data. It is probable, however, that an efficiency higher than 80% is possible.

It can also be seen that the aperture plate temperature is affected slightly by the fluid temperature, while the heat exchanger and cavity temperatures are affected more.

Table 6-3

Summary of Solar Stirling Receiver Test Results

Test No. 3, June 1, 1977

Printer Line Number*	258	307	311	318	355
Time from Start, Minutes	129.0	153.5	155.5	159.5	177.5
Solar Intensity BTU/HR-FT ₂	332	332	329	329	326
Collected Energy Rate, KW	2.11	3.08	3.44	3.20	3.48
He Flow Rate, LBM/HR	73.5	78.5	86.0	80.9	92.9
Gas Inlet Temp., °F	795	903	862	801	652
Gas Outlet Temp., °F	874	1011	972	910	828
Average Tube Temp., °F	949	1011	972	910	744
Average Cavity Temp., °F	1152	1223	1187	1227	1159
Aperture Plate Temp., °F	1416	1460	1451	1451	1416
Receiver Eff., % (Based on 60% Coll. Eff.)	51	74	85	78	87
Receiver Eff., % (Based on 66% Coll. Eff.)	46	68	77	71	79
Radiative Heat Loss, KW	0.07	0.09	0.08	0.07	0.06
Conductive Heat Loss, KW	0.03	0.03	0.04	0.03	0.04
Convective Heat Loss, KW	0.01	0.01	0.01	0.01	0.01

* Line number from paper tape print outs. The start of test is 0.

Table 6-4

Data Points and Description of Conditions
Test No. 3, June 1, 1977

Line Printer*	Time MIN**	Comments
1	0.5	Start, shade up
6	3.0	ΔT increasing
13	6.5	
21	10.5	
26	13.0	
31	15.5	
38	19.0	
47	23.5	
110	55.0	Restart, ΔT increasing, H_s *** fluctuation, 1/2 flow just before heaters on
117	58.5	ΔT increasing, H_s just stabilized
121	60.5	
125	62.5	
126	63.0	ΔT decreasing, H_s dropping
131	65.5	ΔT & H_s fluctuating at low level
138	69.0	ΔT & H_s fluctuating at lower level
147	73.5	ΔT & H_s fluctuating at low level
168	84.0	H_s temporarily peaked
178	89.0	H_s started moving up, just reduced, heaters just off
180	90.0	H_s continued moving up
195	97.5	
199	99.5	Just after max. flow, ΔT & H_s dropping
217	108.5	
231	115.5	
247	123.5	Heaters just on, ΔT & H_s *** just stabilized
249	124.5	
253	126.5	
258	129.0	
265	132.5	Minor H_s fluctuation
266	133.0	Minor H_s fluctuation
279	139.5	H_s decreasing rapidly
296	148.0	H_s temporarily peaked, heaters just off
301	153.3	H_s in the process of stabilizing
307	153.5	
311	155.5	
319	159.5	
340	170.0	H_s just after minor fluctuation
355	177.5	
377	188.5	H_s decreasing rapidly

* Number of paper tape printout from the start of test

** Elapsed time from start of test (mid morning)

*** H_s = Solar Insolation

VII. ENGINE/ALTERNATOR

The work reported in this section was accomplished during Phase II of this program.

The engine that was designed and fabricated for this project was a single cylinder, free-piston Stirling cycle machine with a bore of 58 mm and a stroke of 25 mm. Helium was used as its working fluid. The engine itself was designed, fabricated and tested by Sunpower Inc., Athens, Ohio, under subcontract to Mechanical Technology Inc. (MTI), Latham, New York. MTI provided materials and engineering consultation to Sunpower and specified several changes to the engine design which were intended to enhance its performance and reliability. The changes were not altogether successful because of the shortness of the contract period, wherein the engine was to have been designed, fabricated and tested in six months. MTI then planned to add the alternator, test the combination, and deliver a complete system to JPL. However, the engine was not delivered on schedule. Repeated dismantling and reassembly were required to make changes, and to adjust the gas bearings and the displacer piston axial positioner. After many attempts at adjustment, the displacer gas bearing effort was finally terminated, and the displacer was subsequently allowed to operate during acceptance tests on chrome-oxide-on-steel bearing surfaces without gas pressure.

The problem of the axial positioning of the displacer was solved by adding pressure ports in the cylinder bore to limit travel of the displacer, an approach that had been used in several earlier engines, but which MTI had hoped to replace in the JPL engine. MTI accepted the engine without the advanced displacer positioner or the displacer gas bearings. The engine had been bench tested for 50 hours at various power levels with a hydraulic engine output load used during the test.

The engine was attached to the alternator at MTI. The alternator, designed and fabricated by MTI, had also not performed as desired and several problems were experienced during its bench test. In addition, specified wire size could not be wound on the alternator stator and a smaller wire had to be used, with a resulting increase in resistive loss in the winding. Also the magnetic poles in the alternator were not positioned correctly, and lead-in wires were broken in test. The shaker which provided the mechanical input to the alternator was incapable of driving the alternator to full stroke, and test data indicated that the alternator stroke would have to be lengthened to obtain the desired output power.

When the engine and alternator were tested together, the alternator plunger was supported by and moved in resonance with the plunger gas spring, as designed. However, the 10.5 lbm plunger caused a 300 watt loss within the gas spring, far more than had been expected. The loss had not been observed in the test of the alternator alone because that test did not involve a gas spring. When the alternator was installed on the engine, the gas spring was essential to its operation.

As an assembly, the engine/alternator system exhibited good efficiency (18-21%), although not as good as had been projected (25%). The engine/alternator was easily started by electrical motoring. Design, fabrication, and test had proven more difficult than expected, but the completed engine/alternator system demonstrated a practical thermal-to-electrical conversion system.

Details of the engine/alternator design and performance are given in the MTI final report which is included herein as Appendix A.

REFERENCES

1. Selcuk, M. K, Wu, Y. C., Moynihan, P. I., Day, F. D. III, "Solar Stirling Power Generation: Systems Analysis and Preliminary Tests," International Solar Energy Society, Solar World Conference, Orlando, Florida, June 6-9, 1977.
2. Selcuk, M. K., Moynihan, P. I., Wu, Y. C., Day, F. D. III, "Solar Stirling Experiments," presented at the Izmir International Symposium on Solar Energy, Izmir, Turkey, August 2-5, 1977.

APPENDIX A

MTI 79TR71

**1-kW SOLAR STIRLING ENGINE-ALTERNATOR
FINAL TEST REPORT**

**Prepared by:
George Dochat**

September 1979

**MECHANICAL TECHNOLOGY INCORPORATED
968 Albany-Shaker Road
Latham, New York 12110**

TECHNICAL REPORT

**1-kW SOLAR STIRLING ENGINE-ALTERNATOR
FINAL TEST REPORT**

George R. Doehat

Author (s) George R. Doehat
Bruce Goldwater

Approved Bruce Goldwater

Prepared for
Jet Propulsion Laboratory

Prepared under
Contract No.
954838

PRECEDING PAGE BLANK NOT FILMED



MECHANICAL TECHNOLOGY INCORPORATED

968 ALBANY - SHAKER ROAD - LATHAM, NEW YORK -- PHONE 785-0922

TABLE OF CONTENTS

<u>Section</u>	<u>Page</u>
LIST OF FIGURES	iii
LIST OF TABLES.	iii
1.0 INTRODUCTION.	1-1
1.1 Requirements	1-1
1.2 Summary of Results	1-2
2.0 FREE-PISTON STIRLING ENGINE TEST.	2-1
2.1 Description of the Hardware.	2-1
2.2 Test Quantities.	2-3
2.2.1 Instrumentation List.	2-4
2.3 Results.	2-7
3.0 LINEAR ALTERNATOR	3-1
3.1 Description of the Alternator.	3-1
3.1.1 Stator.	3-1
3.1.2 Plunger	3-1
3.2 Test Quantities.	3-3
3.3 Results.	3-4
4.0 FREE-PISTON STIRLING ENGINE - LINEAR ALTERNATOR SYSTEM. . .	4-1
4.1 Description of the System.	4-1
4.2 Test Quantities	4-8
4.2.1 Test Equipment-Instrumentation.	4-9
4.2.2 Test Plan	4-15
4.3 Test History	4-15
4.4 Test Results	4-15
5.0 CONCLUSIONS	5-1
APPENDIX A - TEST PLAN AND PROCEDURES.	A-1

PRECEDING PAGE BLANK NOT FILMED

LIST OF FIGURES

<u>Figure No.</u>		<u>Page</u>
2-1	JPL Engine Layout	2-2
2-2	1 kW Free-Piston Stirling Engine.	2-8
2-3	JPL Engine Thermocouple Identification.	2-10
2-4	Displacer Number One.	2-11
2-5	Displacer Number Two.	2-12
3-1	Section View of JPL Alternator.	3-2
3-2	JPL 1 kW Linear Alternator.	3-5
3-3	JPL Alternator Efficiency versus Load Resistance.	3-6
3-4	JPL Alternator Power versus Field Voltage	3-7
3-5	DOE Design III Alternator 60 Hz Test Performance. (75 μ f series capacitance)	3-8
4-1	JPL System Layout	4-2
4-2	JPL Displacer and Power Piston.	4-3
4-3	JPL Alternator, Plunger and Power Piston.	4-4
4-4	JPL System Components	4-5
4-5	JPL Test Cell and Operator's Console.	4-6
4-6	MTI Free-Piston Stirling Engine Laboratory. (JPL engine in right-hand test cell)	4-7
4-7	Engine/Alternator System Instrumentation Schematic.	4-7
4-8	1 kW Solar Engine/Alternator ac Power Output versus Stroke at 650° and 60-80 bar	4-21

LIST OF TABLES

<u>NUMBER</u>		<u>PAGE</u>
2-1	JPL Engine Run Data (Displacer Configuration Number One)	2-9
2-2	JPL Engine Run Data (Displacer Configuration Number Two)	2-13
4-1	Type K Thermocouples.	4-11
4-2	Engine Operation Instrumentation.	4-12
4-3	Summary of Major Test Points.	4-16

1.0 INTRODUCTION

Mechanical Technology Incorporated (MTI), under contract to the Jet Propulsion Laboratory (JPL), designed, fabricated, and tested a free-piston Stirling engine/linear alternator system. This energy conversion system was proposed to be delivered to JPL for integration with a solar collector/receiver designed and developed by JPL for solar demonstration testing. The contract required that, prior to delivery of the system, MTI demonstrate the capability of the system to meet JPL specifications by testing the engine, alternator and engine-alternator system. This report contains the test results of the component tests performed at MTI.

1.1 Requirements

The requirements specified by JPL for the free-piston Stirling engine/linear alternator were designated as follows:

Free-piston Stirling engine will:

- Be created as a developmental prototype
- Operate trouble free
- Achieve an efficiency goal of 30%
- Maintain heater head temperatures within 1000 to 1200°F
- Develop without having engine weight and envelope being first-order considerations

Alternator will:

- Achieve an efficiency goal of 88%
- Operate at 30 Hz
- Operate at 1 kW_e output

Free-piston Stirling engine-linear alternator system will:

- Have capability of being hermetically sealed
- Achieve an efficiency goal of 25%
- Reach nominal output of 1 kW_e.

In addition, the design had to interface with an existing JPL solar receiver.

1.2 Summary of Results

Testing of the free-piston Stirling engine/linear alternator and engine-alternator were completed successfully. The engine demonstrated sufficient power (~1400 watts) and exceeded the efficiency goals established for this program.

Because of problems encountered during fabrication of the linear alternator, this unit did not achieve the efficiency goal of 88% but was only 81% efficient. Based on known problems with known solutions, the alternator was judged to be acceptable for engine-alternator and solar demonstrations. The alternator data were extrapolated to show that the alternator was capable of generating 1 kW electric output.

After solution to some initial development problems, testing of the engine-alternator system was performed. The engine-alternator system has proved to be a reliable, rugged system during the testing program. With further system characterization testing, this engine-alternator system could be incorporated with a solar receiver and be used for solar conversion demonstration. At design stroke, the system provided a total ac power output of 870 watts at an overall system efficiency of 20% (heat input to ac power output), while peak power obtainable was 932 watts at 6% overstroke. The frequency of the system was at the design value of 30 Hz.

With the successful completion of initial system testing, MTI is confident that the utilization of free-piston Stirling engine/linear alternators can be realized in highly efficient, reliable energy conversion systems such as a solar system.

2.0 FREE-PISTON STIRLING ENGINE TEST

2.1 Description of the Hardware

The design of the free-piston Stirling engine was performed by MTL/Sunpower. The major design parameters established for this engine were:

Engine efficiency	30%
Heater head temperature	650°C
Engine shaft power	1350 watts
Piston stroke	2.54 cm
Engine frequency	30 Hz
Charge pressure	70-80 bar

A schematic of the engine is shown in Figure 2-1; the engine assembly drawing is found in the back cover of this report. The testing of this engine was performed at Sunpower Inc. and the power output of the engine was dissipated in a load device.

The detail design of the engine heat exchangers is as follows:

Heater Characteristics

34 tubes
Length = 18.34 cm
Inner diameter = 2.362 mm
Flow area = 1.49 cm²
Wetted perimeter = 25.23 cm

Regenerator Characteristics

Annular regenerator
Outer diameter = 7.118 cm
Inner diameter = 6.07 cm
Length = 5.84 cm
Matrix mass = 60.5 gm
Matrix material = 304 stainless steel 100 x 100 mesh woven screen
Wire diameter = 25 E-6 mm
Porosity = 88.8%
Canister volume = 67.32 cc

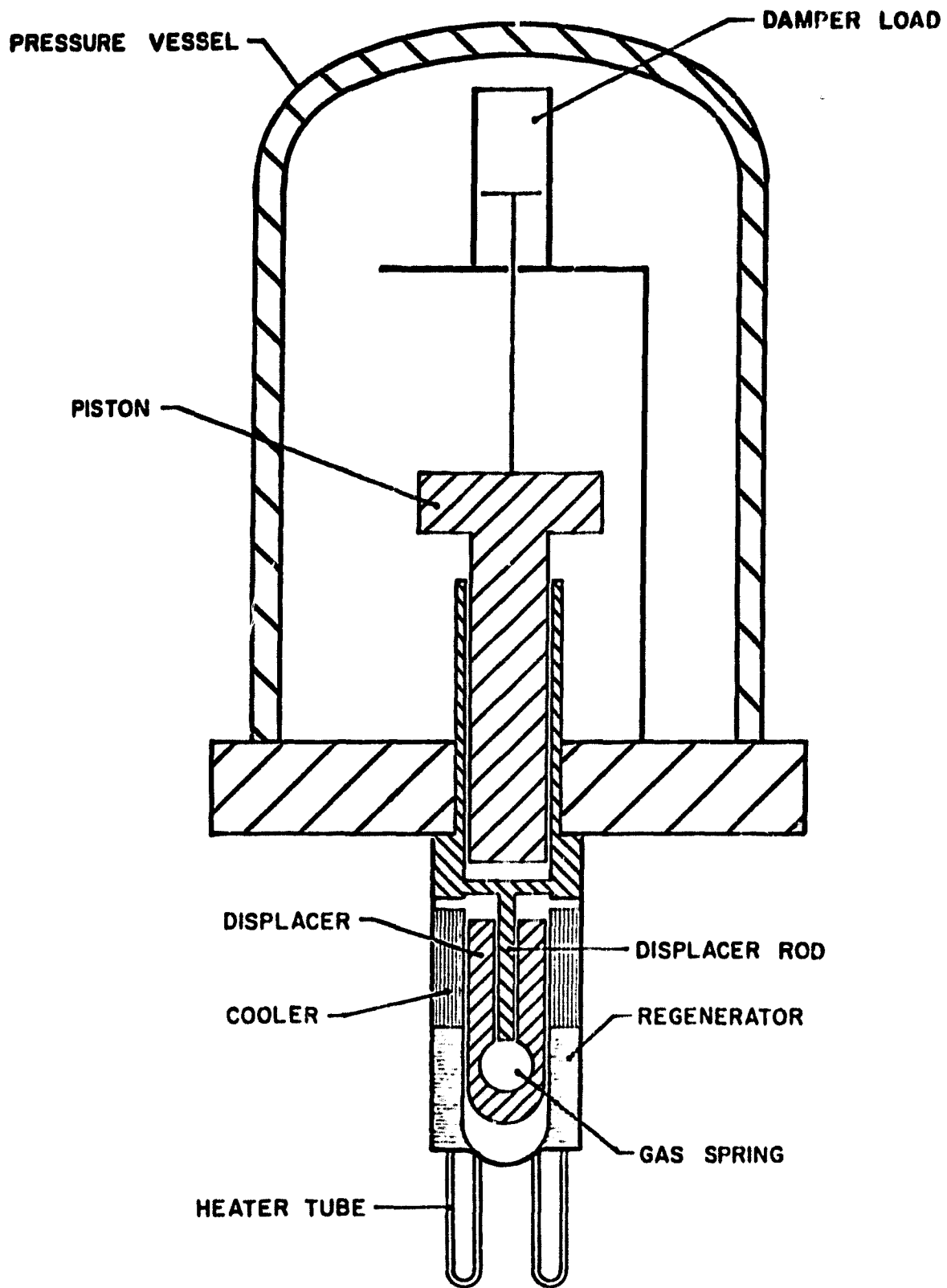


Fig. 2-1 JPL Engine Layout

Cooler Characteristics

135 rectangular passages

Passage width = .0508 cm

Passage depth = .376 cm

Length = 8.45 cm

Flow area = 2.58 cm²

Wetted perimeter = 115.2 cm

Volume = 21.77 cc

System Characteristic

Piston and displacer diameter = 2.25 in.

2.2 Test Quantities

The heat source for the engine will eventually be solar irradiation supplied by a solar collector designed and tested by JPL. For the purposes of testing the engine at Sunpower and engine-alternator at MTI, however, the heat source was an electrical heater head. The electrical heater head was designed to match the heat input that would be available from the solar collector.

The primary purpose of engine testing was to determine the performance map of the engine. The performance was determined at various heater head temperatures, cooler temperatures, and load. The simulated load device is a gas compressor with helium as the working fluid. The performance parameters are the engine output power and the efficiency at which this output power can be delivered. Consequently, it was necessary to measure the electrical power input, heat losses from the heater, the heat which was rejected from the engine and transferred to the cooler, load dissipated in the load device, and the dynamic positions, pressures, velocity and force of the displacer and power piston. The test was performed with an electric heater head and a simulated load. During each test run, the engine was charged with helium up to the design pressure, cooling water applied, and power added to the electric heater. The start temperature and time required to reach design power and steady-state operation was also recorded. Once steady-state operating conditions were reached, the following was recorded:

- a) cooling water flow rate, ΔT and Y
- b) pressure-volume trace
- c) frequency
- d) force-position trace or force-velocity
- e) piston and displacer position versus time (i.e., stroke)
- f) pressure and force to load versus time
- g) wall temperature of heater, regenerator, and cooler
- h) power delivered to external load

Testing was conducted over a range of heater wall temperatures at maximum power loading for each point, and at 80% of maximum power as set by the loading device. The test data was analyzed and a performance map of the engine and a table of run results were prepared.

2.2.1 Instrumentation List

The JPL 1 kW free-piston Stirling engine is outfitted to measure the six parameters identified in this subsection. All appropriate transducers are supplied with the engine and require pressure wall feed-throughs.

- Dynamic Working Space Pressure
 - Transducer: Kistler #211B2 quartz pressure transducer
 - User Interface: 10-32 microdot receptacle
 - Accessories Required: Kistler 128M cable
Kistler 504E charge amplifier or equivalents
- Dynamic and Static Bounce Space Pressure
 - Transducer: Kristal #4075 A100 Piezoresistive pressure transducer
 - User Interface: Kristal 4-pin connector
 - Accessories Required: Kristal #4753SP7
Kristal #4601 Piezoresistive amplifier
or equivalent
- Expansion Space Temperature
 - Transducer: CAIN-116E C rga thermocouple
 - User Interface: Chromel-alumel Omega miniature connector (supplied with the engine)

● **Piston Load Force**

Transducer: Kistler #923F1 Piezotron heavy duty load cell with adapters

User Interface: 10-32 microdot receptacle

Accessories Required: Kistler 121M(X) cable
Kistler 504E charge amplifier or equivalent

● **Piston Velocity**

Transducer: Transtek #112-001 linear velocity transducer

User Interface: two each AWE #22 wires

Accessories Required: none

● **Displacer Relative and Piston Absolute Position**

Transducers: Transtek #244-000 dc-dc LVDT with capacitive filter on output removed

User Interface: Output: 2 each AWG #22 wires for each transducer

Input: 2 each AWG #22 wires for each transducer

Accessories Required: Output: 2nd order low-pass filter with -3 db = 300 Hz for each transducer
Input: 5.6V dc power supply

The signals from these transducers interfaced with Sunpower's data acquisition system in a manner that makes data available as follows:

1. **Bounce Space Pressure** - The Kristal Piezoresistive pressure amplifier provides a signal to a digital voltmeter which displays static pressure in bars. This pressure is recorded on a data sheet.
2. **Frequency** - The dynamic pressure of the working space signal from the Kistler charge amplifier is fed to a digital Hewlett-Packard, hp frequency counter. The frequency data are recorded on a data sheet.
3. **Power Output** - Both the force to the load signal and the piston velocity signal are fed to a multiplier circuit which determines the stroke x velocity (F-S) power output and displays it on a digital meter. This output is recorded on a data sheet. The

dynamic working space pressure and the velocity are also fed to the integrator, yielding the pressure x volume (P-V) power. This measurement also is displayed and recorded. The power output signal is fed to a light beam oscillograph to be recorded with the dynamic signals.

4. Phase Angles - Signals of the piston position, displacer relative to the piston position, and dynamic working space pressure are all fed to a circuit which displays phase angle or the pressure phase angle. These signals are recorded on the data sheet.
5. Engine Head Temperatures - Three thermocouples are strategically placed on the heater tubes, and three are placed on the head itself. The signals from these thermocouples are fed into a maximum voltage selector and discriminator circuit to insure against burn out. The maximum temperature signal is also fed to an automatic controller which regulates input power. Any of the six thermocouples or the maximum voltage circuit output can be displayed on a digital meter. They are recorded on the data sheet.
6. Coolant Flow - Coolant flow rate is measured with an in-line rotometer. The flow rate is recorded on the data sheet.
7. Coolant Temperature Rise - Two thermocouples are arranged to measure delta temperature of the coolant, while a third thermocouple measures coolant inlet temperature. The signals are displayed on a digital meter and recorded on the data sheet.
8. Power Input - The current delivered to the head is measured with two ceramic current transformers. Transformer secondary voltage and the voltage across the head are fed to an integrator circuit, the output of which is displayed on a digital meter and recorded on the data sheet.
9. Dynamic Variables - Signals of the piston position, displacer relative to the position, working space pressure, and force to the load are all fed to a light beam oscillograph which displays them as a function of time. A section of the display is attached to the data sheet. These signals are also fed to two oscilloscopes which display a phasing plot and a pressure volume plot or force

position plot. Photos of these plots are taken and attached to the data sheet.

2.3 Results

During initial testing of the engine, problems were encountered with the method used to control the displacer and also the displacer gas-bearing system. The displacer control system "blips" small amounts of helium in or out of the displacer gas springs in order to keep the displacer centered. However, because of large volume and lag time associated with the control system, the displacer would drift from one stop to another without being centered. The solution to this problem was to center the displacer using a porting arrangement that connects the gas spring and mean engine working pressure.

The second major problem was that the displacer gas bearings were a source of contamination and eventual damping of the displacer. To avoid this problem, a decision was made to operate the engine without gas bearings on the displacer. Judgment was based on observation of the excellent wear characteristics of the chrome oxide displacer rod operating against the hardened steel displacer bore.

After solving these two major problem areas, the engine was operated for approximately 50 continuous hours. The results are presented as a performance map shown in Figure 2-2. Selected design points are presented in Table 2-1. Head temperature locations are shown in Figure 2-3.

These data were taken with an engine build,utilizing displacer configuration number one shown in Figure 2-4.

Since the displacer stroke was less than desired and because the power output was low at the design stroke, a new displacer rod and displacer were designed and fabricated. This new displacer design is shown in Figure 2-5. The displacer seal was a clearance type on the first configuration and a glass-filled Teflon split-ring type on the second.

The second configuration was tested briefly before the engine was shipped to MTI. The results are shown in Table 2-2. System testing at MTI was performed with the second displacer configuration.

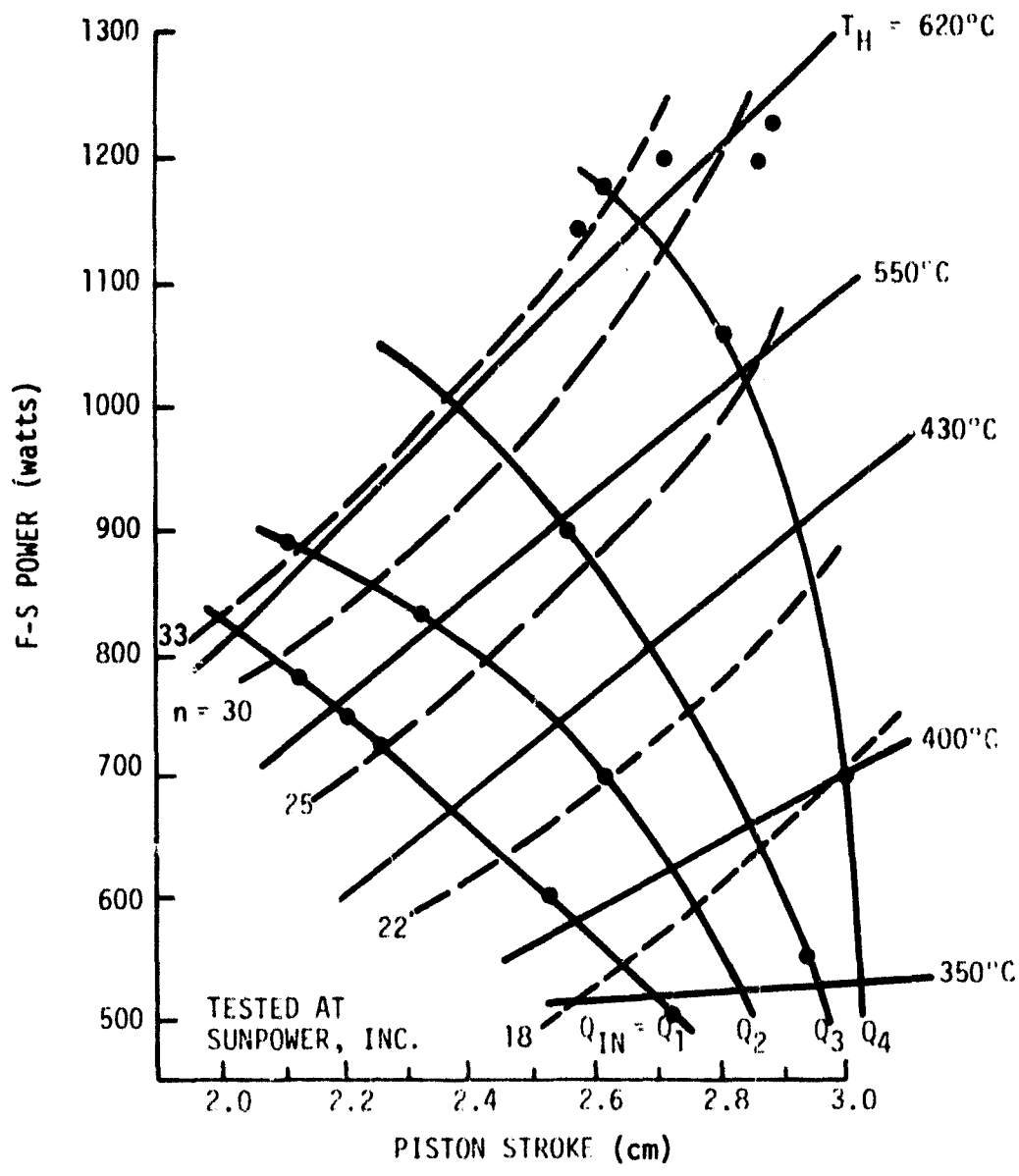


Fig. 2-2 1 kW Free-Piston Stirling Engine

TABLE 2-1

JPL ENGINE RUN DATA

	<u>Displacer</u> <u>Configuration Number One</u>		
Date	9/3	9/4	9/4
Pressure (bar)	72	73	72.6
Frequency (Hz)	29.7	30	29.8
F-S Power Output (W)	1200	850	780
Displacer Phase (°)	49.6	48.9	44
Thermocouple No. 7 (°C)	600	540	530
17 (°C)	470	440	440
18 (°C)	560	520	520
19 (°C)	540	500	500
20 (°C)	560	520	510
21 (°C)		220	
Water Flow (Rotometer)	162	156	155
Water ΔT (°C)	6.55	6.1	5.37
Pressure Phase (°)	-16.5	-18	-19
Power Input (kW)	5.5	4.03	3.70
P-V Power (W)	1140	784	708
Compression Space Gas Temperature (°C)	43.9	36.6	37.8
Piston Stroke (cm)	2.7	2.31	2.12
Displacer Stroke (cm)	2.6	2.25	2.38
Pressure Amplitude (bar)	11.2	8.1	8.6
Efficiency	.33	.29	.30

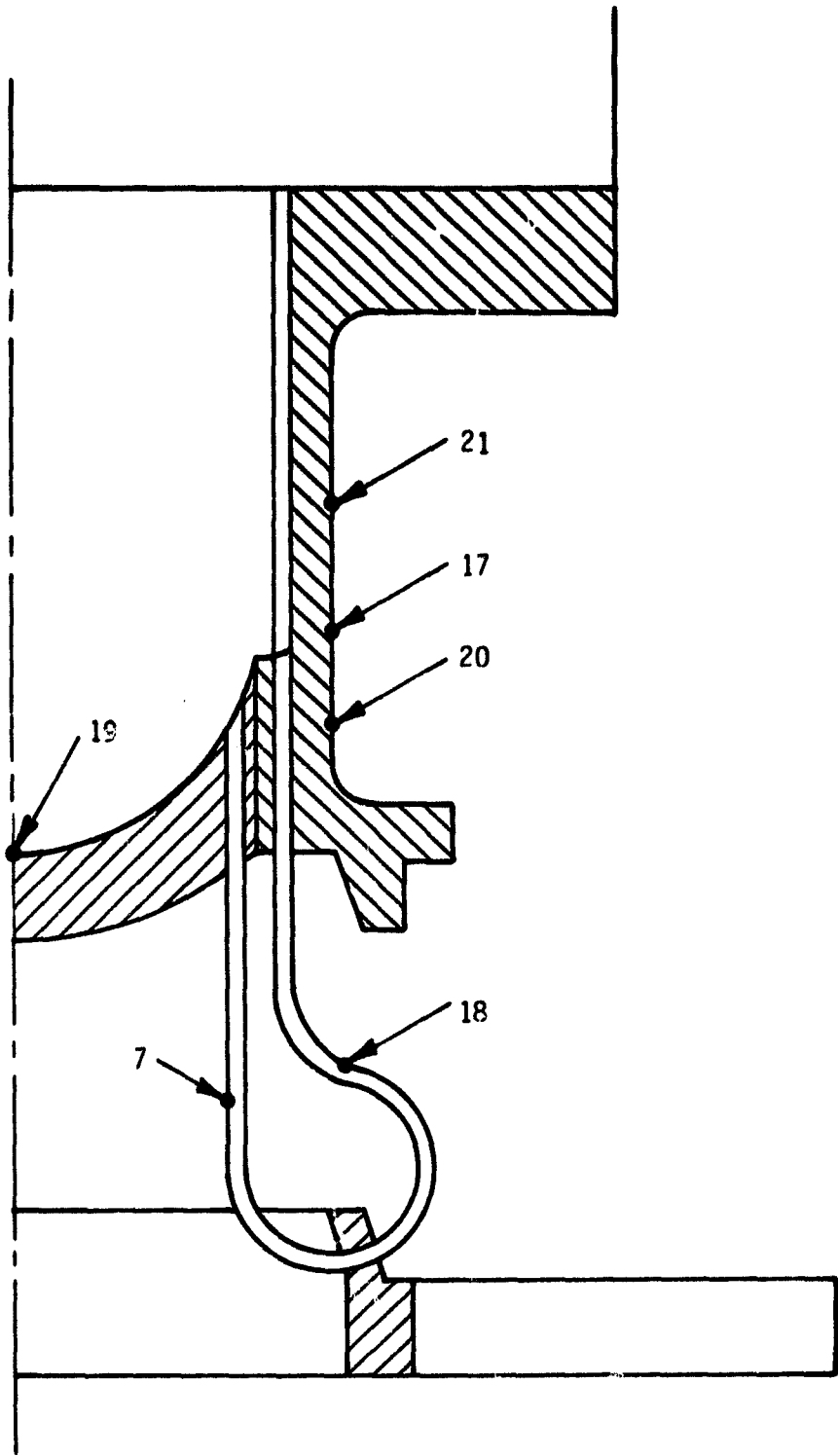
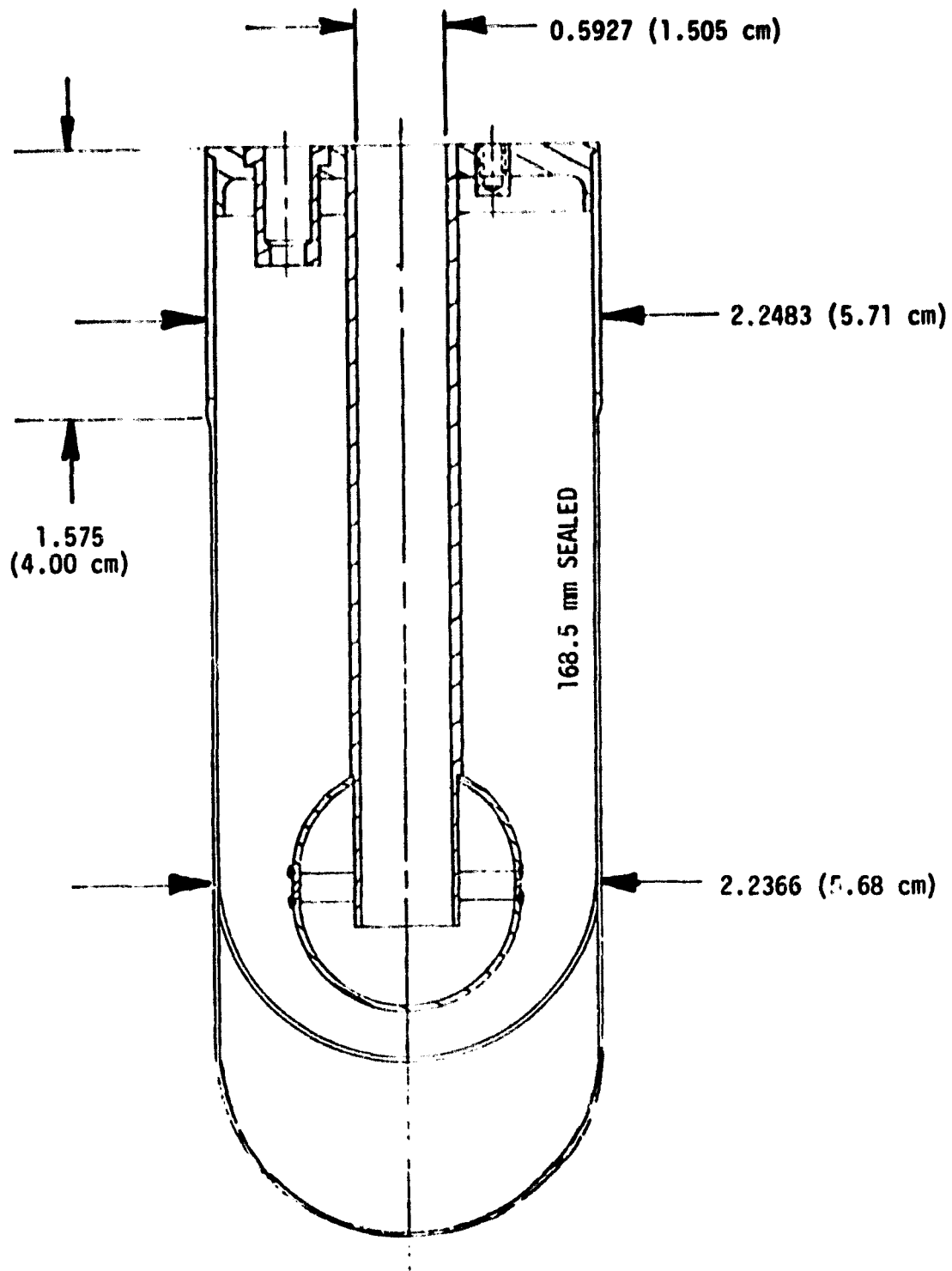


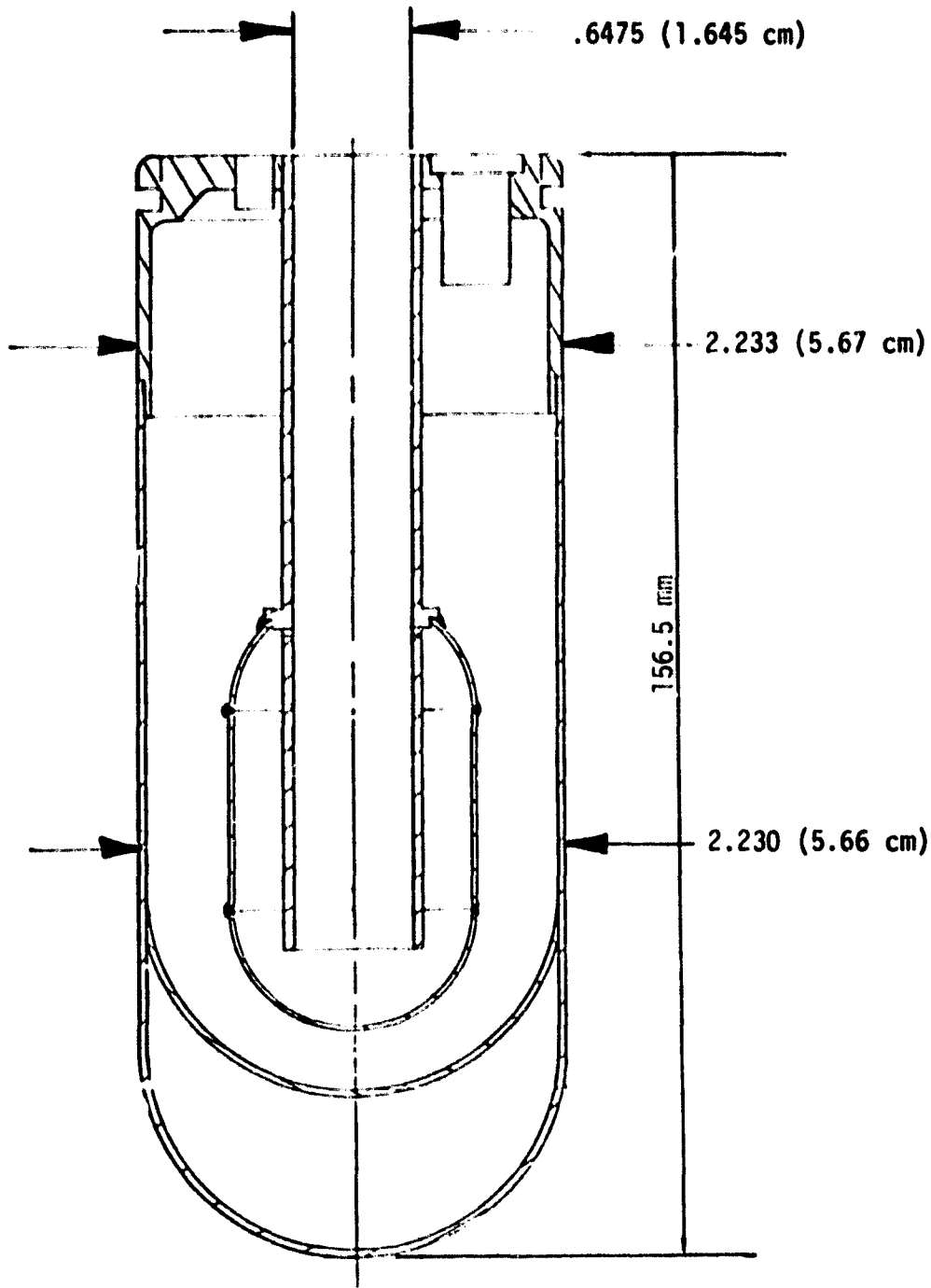
Fig. 2-3 JPL Engine Thermocouple Identification



GAS SPRING MEAN VOLUME 19.4 cc
 GAS SPRING MEAN SURFACE AREA 52.3 cm²

792875

Fig. 2-4 Displacer Number One



GAS SPRING MEAN VOLUME 35.30 cc
 GAS SPRING MEAN SURFACE AREA 97.9 cm²

Fig. 2-5 Displacer Number Two

TABLE 2-2**JPL ENGINE RUN DATA**

Data	<u>Displacer Configuration Number Two</u>	
	9/16	9/16
Pressure (bar)	68	68
Frequency (Hz)	30.2	29.7
F-S Power Output (W)	1150	1100
Displacer Phase (°)	44	44.2
Thermocouple No. 7 (°C)	620	650
17 (°C)	470	500
18 (°C)	590	620
19 (°C)	560	600
20 (°C)	600	610
21 (°C)	180	60
Water Flow (Rotometer)	164	163
Water ΔT (°C)	7.81	7.81
Pressure Phase (°)	-17.5	-22
Power Input (kW)	5.9	6.09
P-V Power (W)	1160	1240
Compression Space Gas Temperature (°C)	58.6	58.6
Piston Stroke (cm)	2.68	2.75
Displacer Stroke (cm)	2.61	2.9
Pressure Amplitude (bar)	11.1	10.6
Efficiency	.29	.28

The engine was judged to be acceptable, based on the power output and efficiency at the design stroke and pressure. The engine was then shipped to MTI.

3.0 LINEAR ALTERNATOR

3.1 Description of the Alternator

The alternator consists of two parts, the stator and the plunger. The dc coil establishes a dc flux in the magnetic circuit. The alternating movement of the plunger varies the flux linkage in the ac coils thus creating an alternating voltage across them.

3.1.1 Stator

The stator consists of 875 laminations arranged radially around the axis of motion. The lamination material is .014-inch Hyperco, a 50-50 iron-cobalt alloy which has high saturation and low losses. There are four ac coils and one dc coil. The two ac coils at either end are connected in series addition, while the pairs are connected in series opposition. This is necessary to obtain an addition of the voltages acting on each coil.

3.1.2 Plunger

The plunger laminations are also made from Hyperco material. The laminations are grounded to a taper to eliminate any space between them at the outside diameter of the plunger. The compensation coils exclude ac flux from the area behind themselves thus increasing the ac reluctance and improving the machine's power factor. A typical alternator (stator-plunger) is shown in Figure 3-1.

The frequency of the power provided is the frequency of the applied motion. This is held constant by providing a resonant system. Output power level is a function of stroke, and dc field strength and power output can be modulated by varying either.

The linear alternator performance parameters are:

Output power	1 kW
Frequency	30 Hz
Terminal voltage	240 volts (1-in. stroke)
Output current	4.3 amps
Efficiency	88%

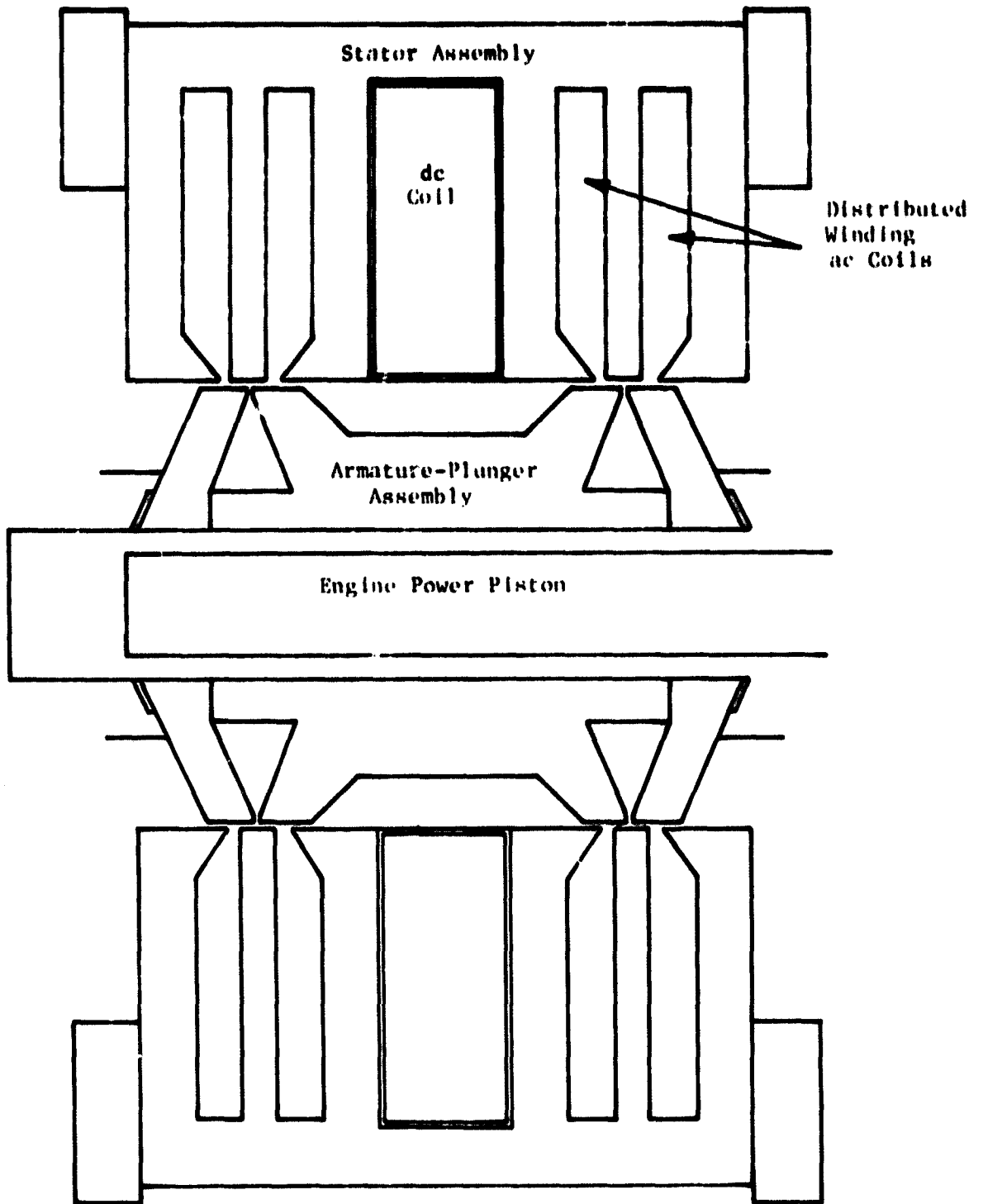


Fig. 3-1 Section View of JPL Alternator

792873

The alternator design parameters for the JPL design are:

Plunger diameter	4.00 in.
Air gap	.030 in.
Stator OD	11.84 ft
Stator width	8.575 in.
dc ampere turns	1600
dc field turns	8000
Stator weight	145 lb
Plunger weight	10.5 lb

3.2 Test Quantities

The derived test quantities of interest are the electrical output power versus the mechanical and electrical input power and the efficiency at which they are accomplished.

The measured quantities are:

- Plunger velocity
- Stator reaction force
- dc voltage
- dc current
- ac voltage
- ac current
- Watts
- Reactive power
- Alpha angle

The mechanical power required to drive the alternator is supplied by a Ling Shaker. Since the Ling Shaker cannot produce platen strokes equal to the required range of alternator plunger strokes, a "motion amplifier" is used in conjunction with the shaker. The motion amplifier provides the correct value of R_a to the system. R_a is the stiffness of the motion amplifier spring pack. It is selected so that the motion of mass, m_p , (which includes the mass of the alternator plunger) will be amplified relative to the motion of the shaker platen.

3.3 Results

The results of the alternator testing are presented in Figures 3-2 through Figure 3-4. It should be noted that the stroke obtained during alternator testing was limited because of spring stiffness of the motion amplifier. A stroke of .8 inch was obtained compared to the 1-inch design stroke. An extrapolation of the data to the design conditions was based on experience with other linear alternators. The main conclusion from the results is that the alternator will provide 1 kW output at or near the design stroke and frequency. The efficiency of the alternator was only 81% versus a design value of 88% when extrapolated to design conditions.

This lower efficiency was most probably caused by:

- 1) The ac coil wire gage size - In order to meet the number of ampere turns required in this design, the ac coil wire diameter was reduced and hence higher losses were obtained. It is estimated that this change would reduce alternator efficiency by 2 percentage points.
- 2) Plunger asymmetry - Due to a manufacturing error, the plunger lamination slots are not symmetric and therefore do not align with stator slots at mid-stroke position. The effect of this error is unknown.

It should be noted that an alternator of similar design to the JPL alternator was built, tested and did exhibit efficiencies of 88 to 90%. The results for this alternator are presented in Figure 3-5.

The JPL alternator was judged to be acceptable for prototype demonstration since power output was adequate and efficiency degradation could be accounted for and explained in any overall system demonstration.

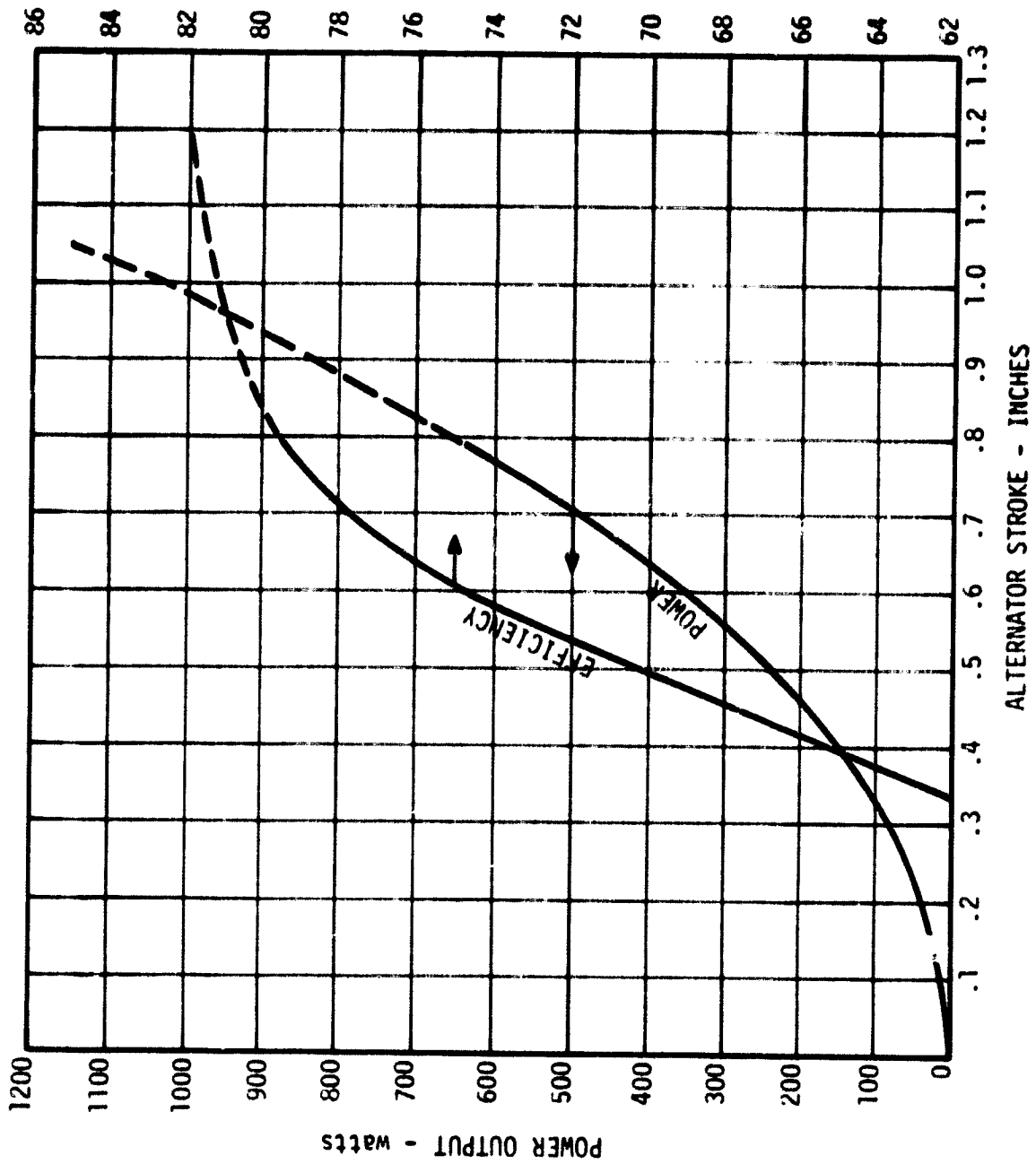


Fig. 3-2 JPL 1 kW Linear Alternator

792552

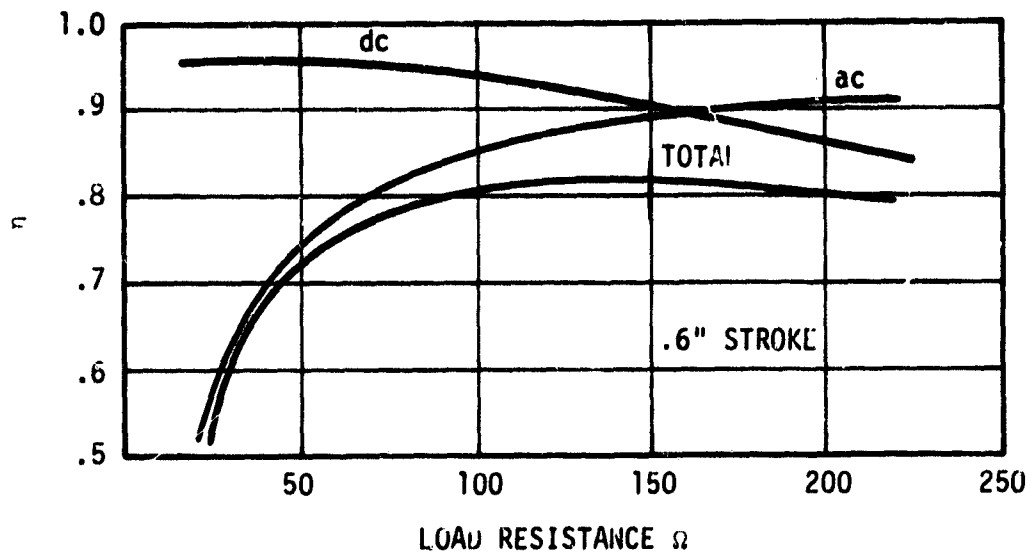
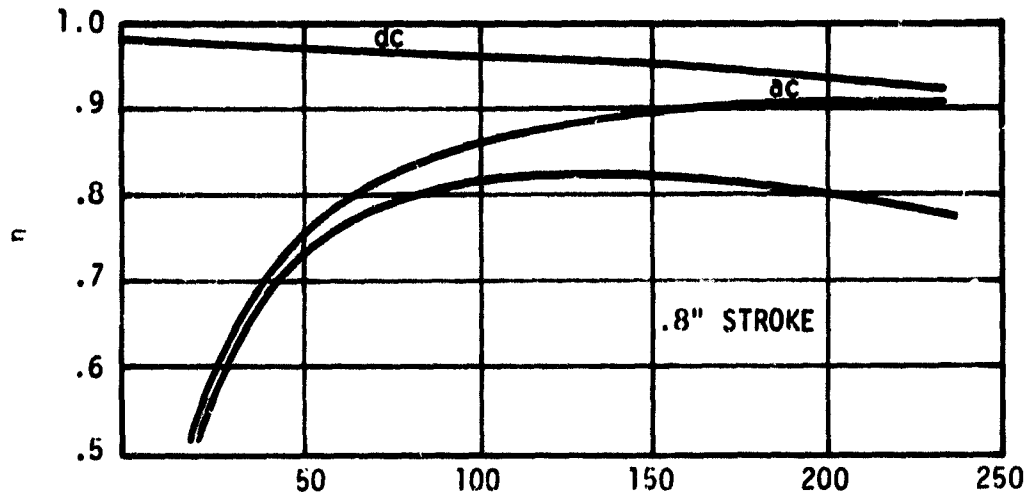


Fig. 3-3 JPL Alternator Efficiency versus Load Resistance

792509

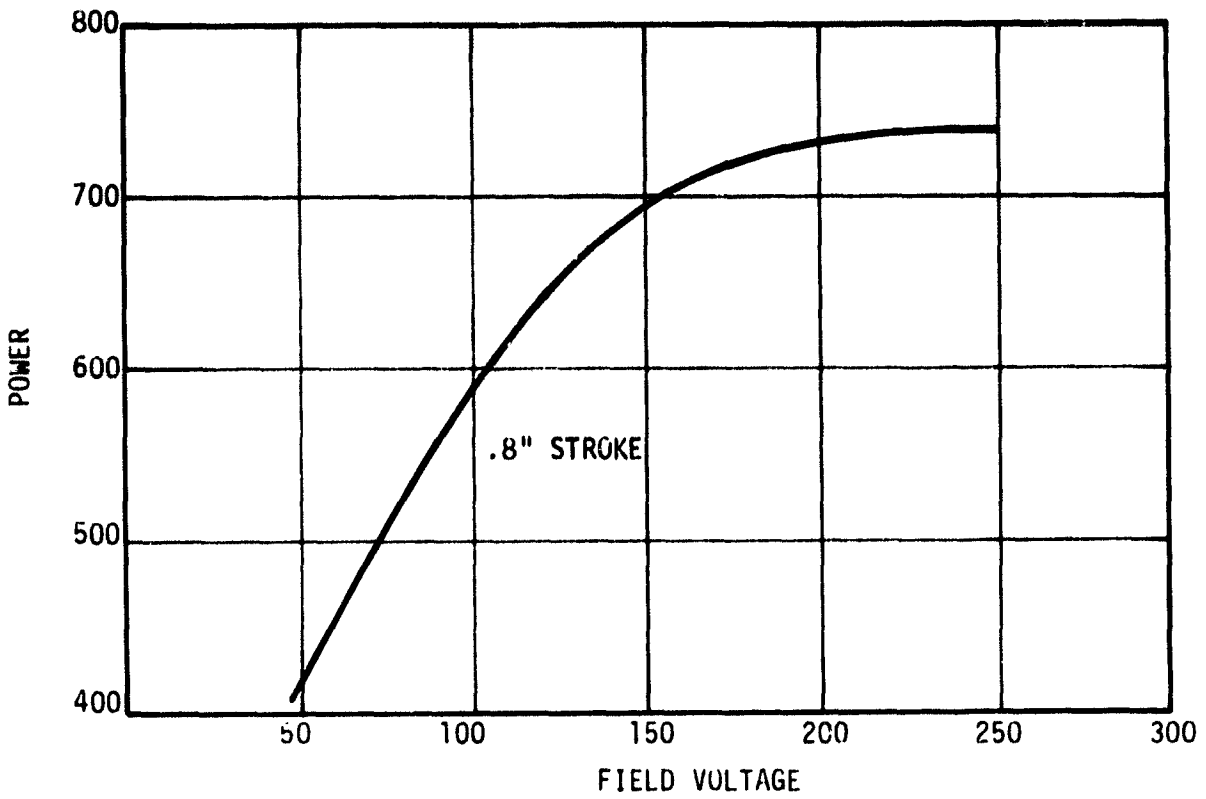


Fig. 3-4 JPL Alternator Power versus Field Voltage

792506

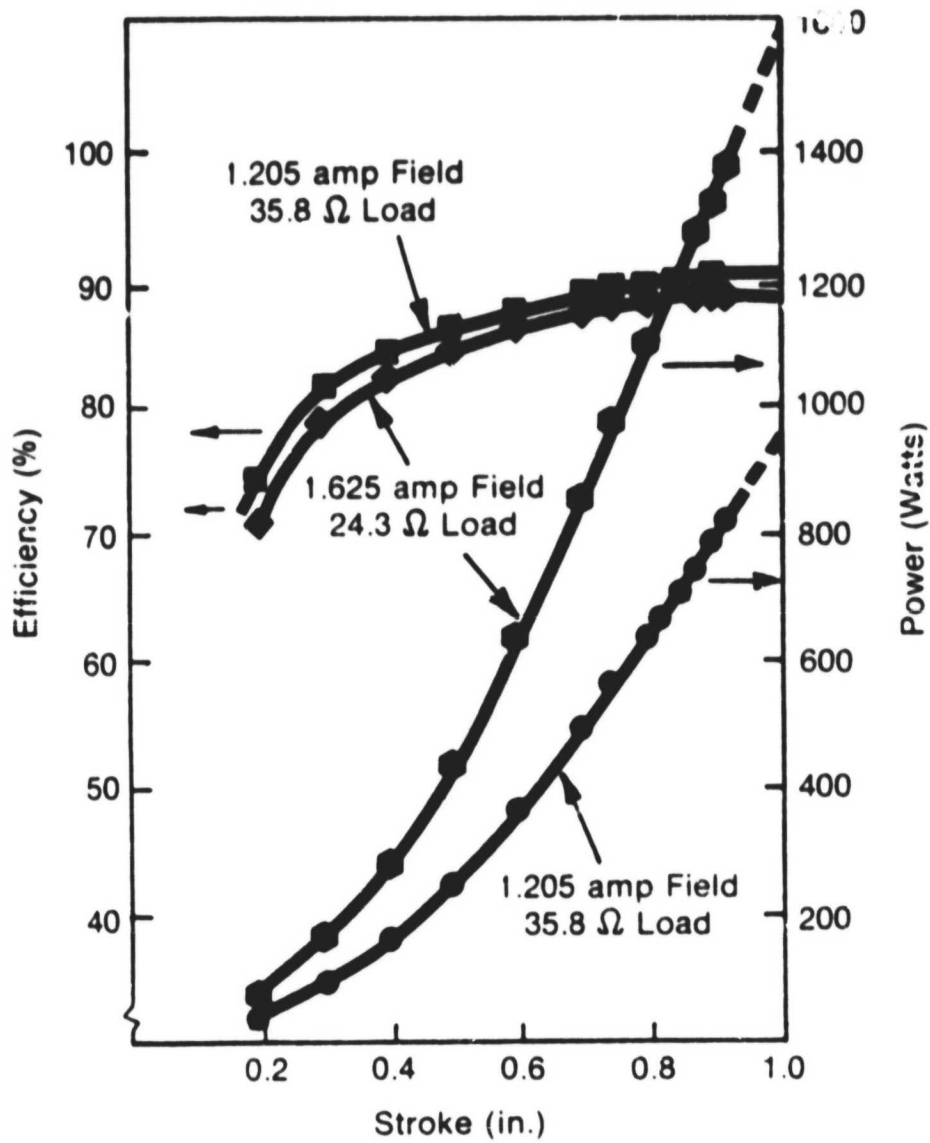


Fig. 3-5 DOE Design III Alternator 60 Hz Test Performance (75 μ f series capacitance)

793551

4.0 FREE-PISTON STIRLING ENGINE - LINEAR ALTERNATOR SYSTEM

4.1 Description of the System

The system represents the integration of the free-piston Stirling engine described in Section 2.0 and the alternator described in Section 3.0. The engine, as received from Sunpower, was dismantled by removing the load device and power piston. It was reassembled utilizing a new power piston, the alternator as the load, and aft gas spring. The engine/alternator layout is shown in Figure 4-1. Photographs of the system hardware and facility are shown in Figures 4-2 through 4-6.

Detail layout of the system hardware as it interfaces with the engine assembly drawing is presented as drawing 384J101 Rev A enclosed in the back cover.

The system design incorporates gas bearings on the power piston and a system to pump the gas bearings internally (during testing of the engine/alternator, bearings were pressurized externally). The system also incorporates a gas spring to maintain frequency at the design point of 30 Hz and sufficient instrumentation to measure desired parameters including orbital position of the piston (i.e., check of gas bearing operation).

The design requirements established for the engine-alternator system as compared to actual test results are presented below:

	<u>Design</u>	<u>Test Results</u>
Power output - system -	1 kWe	870 watts
Frequency -	30 Hz	29.8 Hz
Stroke -	2.54 cm	2.60 cm
Pressure -	70 bar	70 bar
Heater head temperature -	650°C	640°C
Engine efficiency -	30%	33.8%
Alternator efficiency -	88%	81%
System efficiency -	25%	20.6%

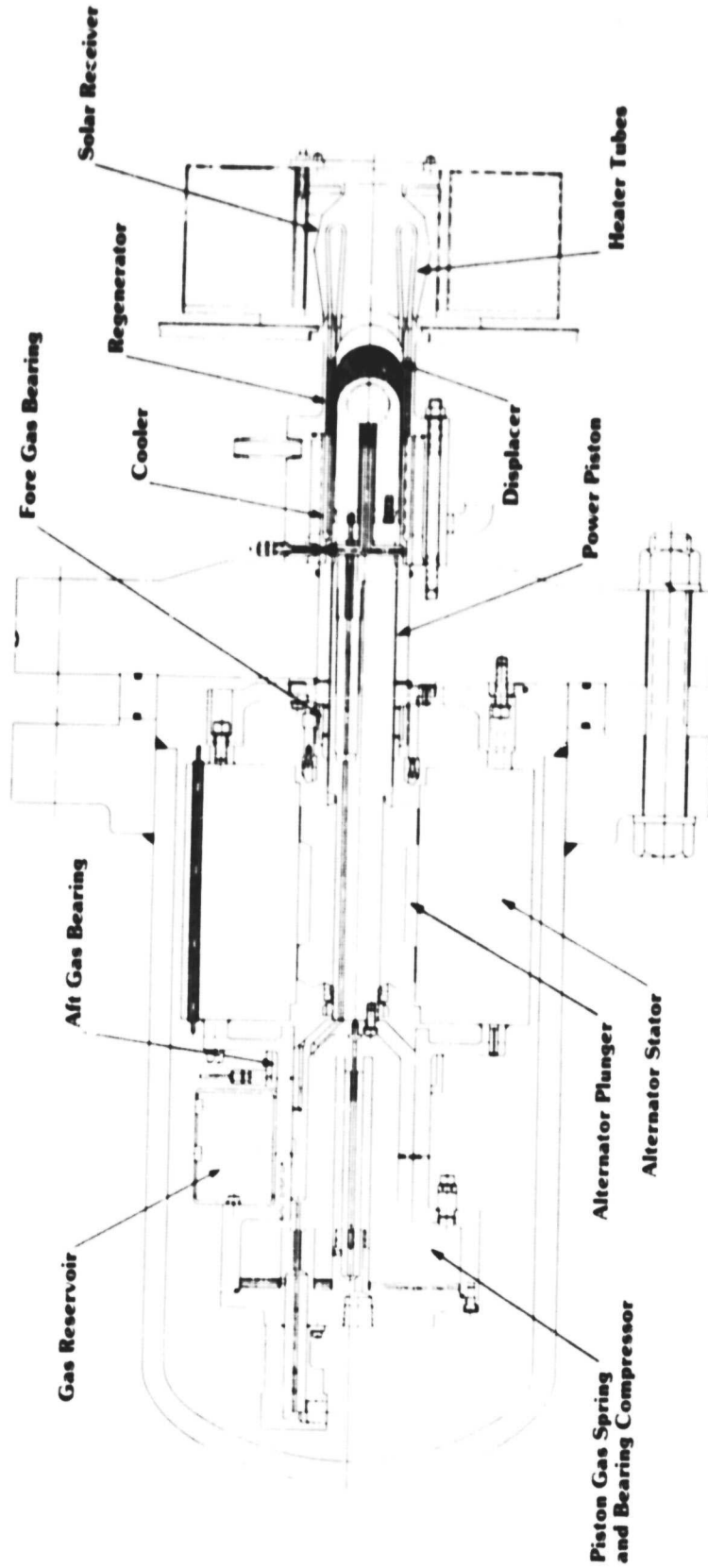


Fig. 4-1 JPL System Layout

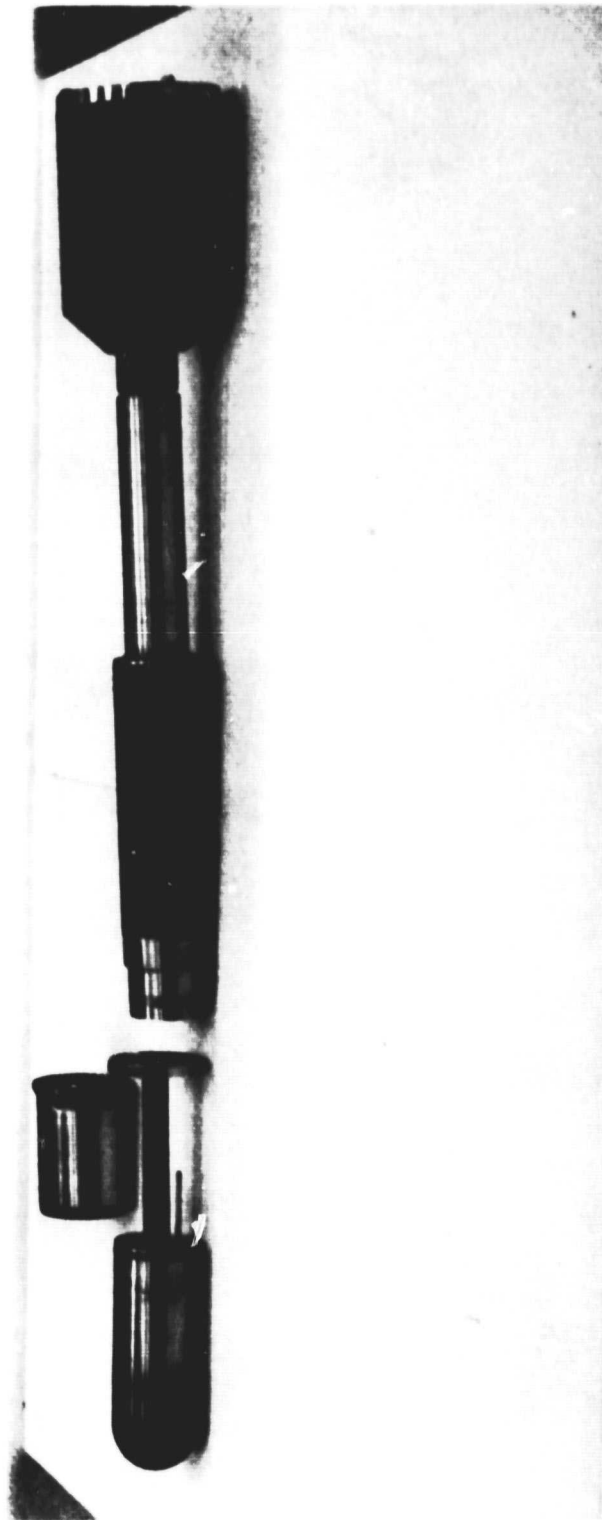


Fig. 4-2 JPL Displacer and Power Pistol

MTI-19126

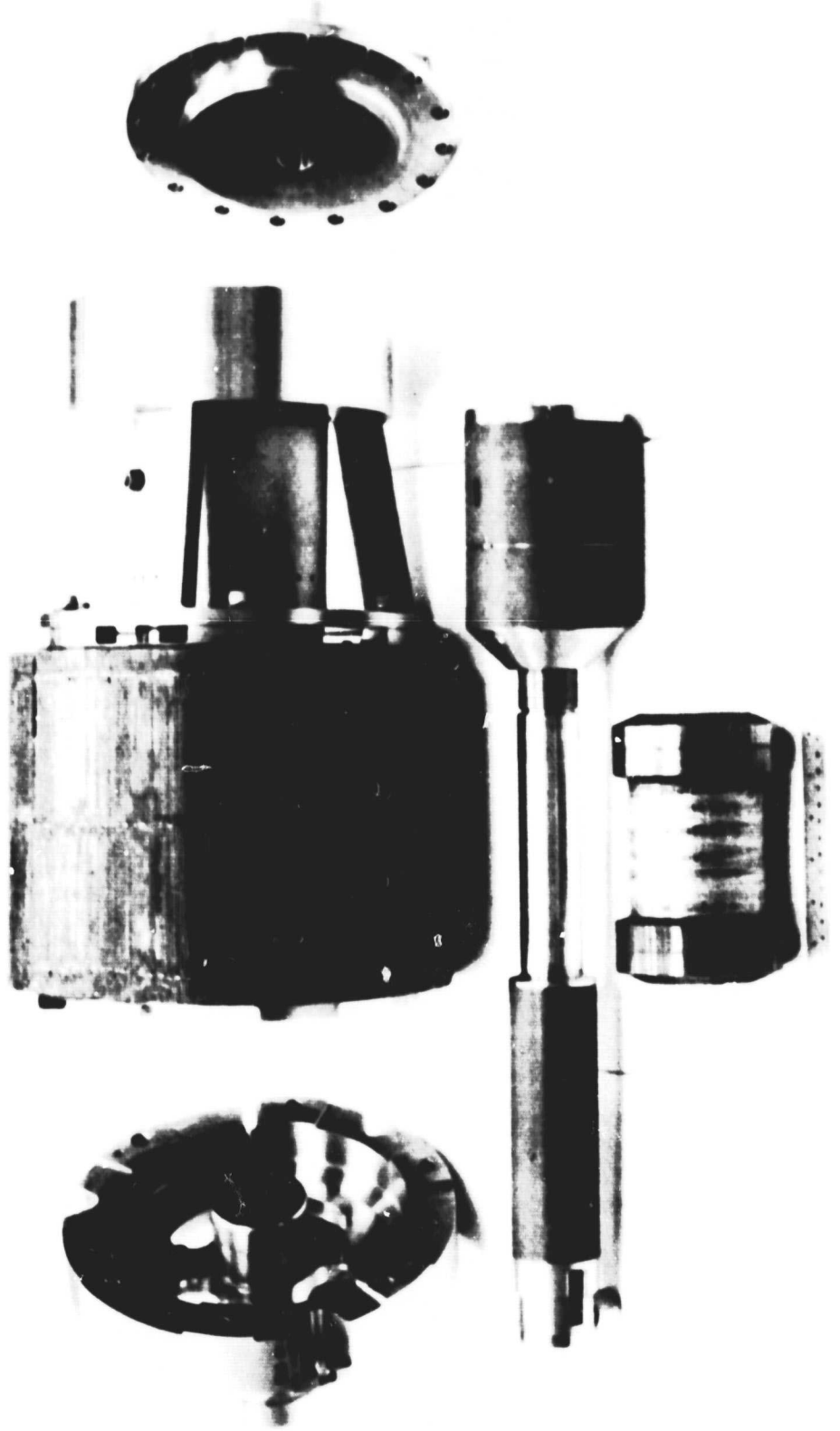
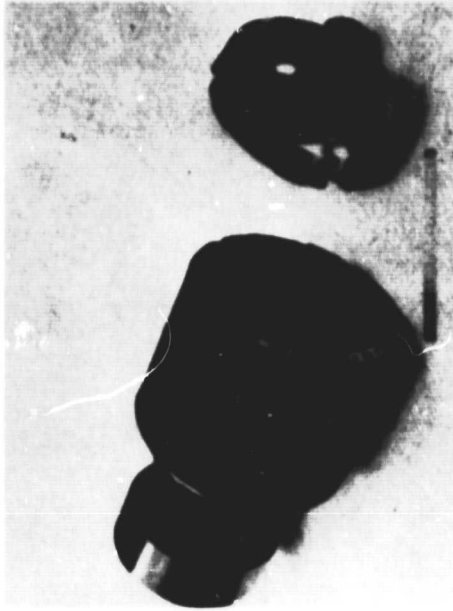


Fig. 4-3 JPL Alternator, Plunger and Power Piston

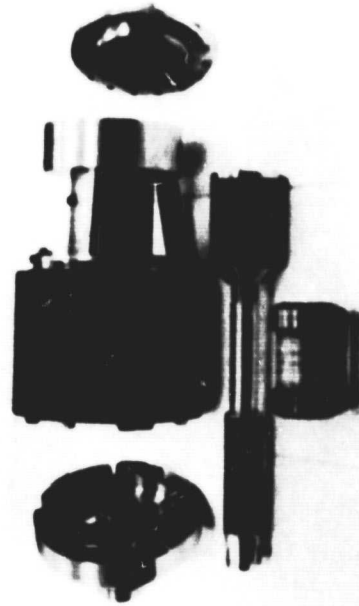
**JPL Stator, Aft Piston Cylinder
and Gas Spring**



JPL Stator and Power Piston Cylinder



**JPL Power Piston Shaft and
Alternator Plunger**



JPL System Components



Fig. 4-4 JPL System Components



Fig. 4-5 JPL Test Cell and Operator's Console



Fig. 4-6 MTI Free-Piston Stirling Engine Laboratory
(JPL engine in right-hand test cell)

MTI-19127

4.2 Test Quantities

The primary independent test variables are:

- Load Demand (i.e., load resistance)
- Field Current
- Temperature

The first two variables are of primary importance for evaluating the interaction between the engine and the alternator performance. The data which are measured or calculated at various operating conditions are:

- Stroke
- Frequency
- Engine power
- Displacer phase and stroke
- Alternator output power
- Alternator output voltage
- Alternator output current and phase
- Output wave forms
- Heat input
- Heat rejected
- Power input to field coil
- Efficiency
- Running time
- Engine starts
- Working space pressure amplitude and phase

The general performance characteristics of the engine and alternator operating separately are fairly well known based on earlier testing.

During testing, the alternator output is dissipated in a resistive load and the current and voltage measured in order to calculate power output. Stator force cells measure electromagnetic gap, external gas spring, and bearing friction forces. This force measurement, along with a plunger velocity measurement, is used to calculate power input to the alternator.

Since the purpose of this test is to confirm the performance of the engine/alternator assembly, the test quantities of interest are the electrical output power as a function of the total mechanical and electrical input power and the efficiency at which the output power is delivered. It is desirable to know the efficiencies of the engine and alternator as separate quantities and, of course, the overall system efficiency.

Basically, the same instrumentation from the separate engine and alternator tests is used to determine the necessary test parameters. The alternator will have a variable dc field and a variable load.

The engine output power (i.e., alternator input power) is determined by the stator force cells and plunger velocity as above. The test is performed with an electric heater head.

4.2.1 Test Equipment-Instrumentation

A system instrumentation schematic of the engine/alternator is shown in Figure 4-7.

Table 4-1 identifies placement of the Type K Thermocouples and Table 4-2 describes the engine operation instrumentation. The following is a list of the instrumentation for engine input power that is required during testing of the engine/alternator:

- General Radio Varied Auto-transformer
 - E_1 = 480 Vac
 - E_0 = 0 - 480 Vac
 - kVA = 31.2
- Perm Motor Control for Auto-transformer
- Signal Transformers
 - Quantity - 2 in series (240 Vac input each)
 - 480 Vac max input
 - Output - 1000 A @ 3 Vac x 2
 - P_{out} = 6 kVA

TABLE 4-1

TYPE K THERMOCOUPLES (grounded junction)

<u>Thermocouple Number</u>	<u>Location Description</u>
1	Top of Regenerator Flange - 270°
2	Side of Regenerator Flange - 270°
3	Bottom of Regenerator Flange - 270°
4	Upper Surface of Regenerator Wall - 270°
5	Middle Surface of Regenerator Wall - 270°
6	Bottom Surface of Regenerator Wall - 270°
7	Outer Heater Tube - 0°
8	Outer Heater Tube - 90°
9	Outer Heater Tube - 180°
10	Outer Heater Tube - 270°
11	Weld on Support Lug - 0
12	Weld on Support Lug - 90
13	Weld on Support Lug - 100
14	Weld on Support Lug - 270
15	Spare
16	Spare
17	Middle of Outer Regenerator Wall - 345°
18	Inner Heater Tube - 0°
19	Expansion Space Temperature
20	Bottom of Outer Regenerator Wall - 90°
21	Top of Outer Regenerator Wall - 90°
22	Working Space Temperature
23	Cooling Water
24	Cooling Water

TABLE 4-2

ENGINE OPERATION INSTRUMENTATION

Signal	Transducer	Signal Conditioning	Measurement Device
Displacer Position LVDT	Trans-Tek Model #293-000	Matched Carrier/Demodulation System made by MTI with Dis- placer, Relative Piston and Absolute Piston Outputs	Stroke is measured using 2 MTI Peak-to-Peak Reading Meters
Piston Position LVDT	Trans-Tek Model #294-000		
Bounce Space Pressure	Kistler Model 4075A100	Kistler Amplifier Number 4601	dc Digital Voltmeter, Hewlett- Packard 3455A
Velocity	Trans-Tek Model #112-001	1 M Ω Resistance	Output Power Meter Produced by MTI
Shaft Force	3 PCB Piezotronics Quartz Force Rings 202A	Sum of Signals in Parallel to Kristal 5001 Charge Amplifier	Performs vector multiplica- tion of velocity and force to produce output power

TABLE 4-2 (cont'd)

Signal	Transducer	Signal Conditioning	Measurement Device
Temperatures	Type K Thermocouples	Type K Reference Junctions HyCal Model 305 or equivalent	dc Digital Voltmeter with 10u volt resolution, HP3455A or equivalent
Cooling Delta Temperature	2 Type T Thermocouples connected in delta configuration	None	dc Digital Voltmeter with 1u volt resolution, HP3455A or equivalent
Alternator ac Voltage	None	None	ac Digital Voltmeter with response to 10 Hz, HP3455A
Alternator ac Current	.1 Ω Dale Resistor 200 W	None	ac Digital Voltmeter with response to 10 Hz, HP3455A
Alternator dc Voltage	None	None	dc Digital Voltmeter, HP3455A
Alternator dc Current	.1 Ω Dale Resistor 50 W	None	dc Digital Voltmeter, HP3455A

TABLE 4-2 (cont'd)

Signal	Transducer	Signal Conditioning	Measurement Device
Working Space Pressure	Kistler 211B2 Pressure Transducer	Kristal 504E Charge Amplifier	Scope
Input Power Current	2 Midwest Electrical Products 2000 to 5 C.T.'s #6CT120B	2 F.W. Bell Watt Transducers	dc Digital voltmeter HP3455A
Input Power Voltage	None	Outputs connected in series	

- Sensing Current Transformer, Midwest Electrical Products, Inc.
Quantity - 2

- F.W. Bell Watt Transducers
Quantity - 2 outputs in series (i.e., summed)
Input: 10 Vac, 5 A @ 60 Hz
Output: 1 MA dc into 0 - 10 k Ω @ 50 W

4.2.2 Test Plan

The test plan and procedures used are enclosed in Appendix A of this report.

4.3 Test History

After receipt of the engine from Sunpower and solutions found to the one-of-a-kind assembly problems, the first successful test of the engine was completed on November 15th when the engine was run intermittently for 15 minutes. Testing was performed with displacer configuration No. 2 as identified in Subsection 2.3 and without the displacer gas bearings. The system was tested numerous times to evaluate the engine's inability to operate for sustained periods at high temperatures and high stroke. It was established that thermal expansion of the piston and piston cylinder housings, with respect to one another, caused a damping of the engine piston and caused the engine to shut down. After minor modifications, the engine/system was tested over high temperatures, high strokes for sustained periods of time. No further recurrence of the drag problem was observed. Since that time, engine-system testing continued without major problems.

4.4 Test Results

A summary of the major test points is presented in Table 4-3.

Figure 4-8 presents the engine/alternator ac power output as a function of piston stroke at 650°C and 60-80 bar for different field voltages. It should be noted that lower field voltage results in less ac power for a given stroke. Design field voltage is 150 volts.

TABLE 4-3

SUMMARY OF MAJOR TEST POINTS

Test Points Units	Piston Stroke cm	Engine Power W	AC Power W	Pressure bar	Displacer Stroke cm	Head Temp. °C	DC Power V	Efficiency of Engine (η_c) %	Efficiency of System (η_s) %	Frequency Hz
12/18/78 #1	2.08	300.9	38	71.6	2.08	-	19.1	13.2	1.6	31.2
2	1.8	155.2	-	71.8	1.879	-	-	8.	-	31.2
3	1.42	87.4	-	71.6	1.58	225	-	6.7	-	31.2
4	2.05	410.9	157	70.2	2.000	-	38.5	17.6	6.2	30.0
5	1.93	247.8	222	70.2	1.838	-	47.5	11.8	10	30.8
6	1.98	673.7	340	67.8	1.83	-	55	26.9	12.1	32.4
7	2.1	786.8	409	67.6	1.90	-	60	28.5	13.2	34.3
8	2.00	772	397	67.1	1.82	-	60	29.5	13.4	33.9
9	1.93	773.8	403	66.8	1.76	634	62	29.5	13.6	30.1
10	1.896	757	393	66.5	1.75	626	62	29.4	11.5	29.4
11	1.47	514	279	66.3	1.43	527	73	26.2	12.8	31.4
12	2.30	1020	532	67.2	2.02	650	67	32.4	14.8	-
13	2.35	1013	532	67.1	2.06	650	65	23.8	13.8	29.9
14	1.6	384	208	67.1	1.61	408	77	20.8	10.3	29.96
15	1.86	349	168	66.8	1.84	355	149	16.8	7.5	30.1
16	2.36	243	-	66.6	2.27	308	-	10.2	-	30.1
17	2.12	207	-	66.2	2.11	288	-	9.5	-	31.1
18	1.96	175.6	-	66.3	1.98	272	-	9.1	-	30.0
19	1.766	123.6	-	65.9	1.85	245	-	7.6	-	30.6
20	1.733	118.6	-	65.9	1.8	240	-	7.8	-	29.9
21	1.57	95.1	-	65.3	1.70	228	-	6.7	-	31.0
22	1.36	70.6	-	65.2	1.55	212	-	6.4	-	29.9

TABLE 4-3 (Cont'd)

Test Points Units	Piston Stroke cm	Engine Power W	AC Power W	Pressure bar	Displacer Stroke cm	Head Temp. °C	DC Power V	Efficiency of Engine (η_c) %	Efficiency of System (η_s) %	Frequency Hz
12/21/78 #1	2.42	724	392	60.5	2.35	455	74	23.5	12.7	29.7
2	2.51	809	485	60.4	2.40	507	103	24.4	14.6	28.5
3	2.49	900	473	60.7	2.34	550	60	27.6	14.5	28.5
4	2.49	960	534	60.2	2.33	605	69	27.8	15.4	28.3
5	2.49	1035	608	60.2	2.32	650	80.5	28.0	16.5	28.1
6	2.46	1062	676	60.5	2.29	652	88.	28.3	18.0	28.3
7	2.54	1083	625	60.3	2.37	648	80	29.8	17.2	28.1
8	2.21	928	571	60.1	2.07	657	160	29.9	18.4	27.8
9	2.76	1230	728	59.8	2.52	649	90	30.5	18.1	28.2
10	DATA N/G									
11	2.88	1284	648	59.7	2.65	634	60	28.6	14.4	28.3
12	1.86	140	-	60.1	1.98	239	-	8.1	-	28.9
13	2.04	183	-	60.4	2.1	253	-	10.3	-	28.8
14	2.5	234	-	59.9	2.44	278	-	10.3	-	28.9
15	1.42	82	-	59.9	1.62	206	-	6.7	-	28.8
12/22/78 #1	2.35	866	646	60.1	2.40	600	63	28.7	21.4	27.1
2	DATA N/G									
1/11/79 #1	2.48	-	199	70.3	2.37	455	51	-	9.1	30.5
2	1.48	214	4	70.1	1.68	278	36.7	15	0	30.2
3	1.49	215	102.8	69.9	1.68	281	40	15.2	7.2	30.2
4	2.25	1027	628	70.1	2.14	650	142	29.5	18.0	29.6

TABLE 4-3 (Cont'd)

Test Points Units	Piston Stroke cm	Engine Power W	AC Power W	Pressure bar	Displacer Stroke cm	Head Temp. °C	DC Power V	Efficiency of Engine (η_c) %	Efficiency of System (η_s) %	Frequency Hz
1/16/79 #1	2.47	1149	664	75.2	2.36	618	73	26.5	15.3	31.2
2	2.70	1179	810	75.3	2.58	614	115	25.3	17.4	31.3
3	2.61	1053	720	75.0	2.47	558	185	26.7	18.3	31.4
4	2.7	1202	857	75.4	2.52	640	180	26.5	18.9	31.4
5	2.69	1209	835	75.2	2.48	651	113	26.8	18.5	31.3
6	2.53	1216	810	80.2	2.41	660	101	24.9	16.6	31.9
7	2.585	979	721	80.2	2.39	617	69	21.1	15.5	32.1
8	1.18	43	-	80.1	1.38	220	-	3.5	-	32.4
9	1.48	64	-	80.8	1.69	234	-	4.5	-	32.6
10	2.03	68	-	80.3	2.09	277	-	3.3	-	32.4
11	2.00	59	-	80.3	2.05	290	-	2.6	-	32.4
12	2.69	1156	904	80.4	2.43	636	120	23.9	18.7	32.3
13	2.69	1205	931	81.1	2.46	661	193	22.9	17.7	32.4
14	2.66	1273	853	70.1	2.52	625	191	28.9	19.4	29.8
15	2.68	1449	900	70.4	2.55	642	178	30.4	18.9	29.8
16	2.6	1430	871	70.7	2.48	652	151	33.8	20.6	29.8
17	2.79	1400	900	70.5	2.68	652	80	28.5	18.3	29.9
18	2.24	1098	567	70.0	2.16	622	150	28.3	14.6	29.4

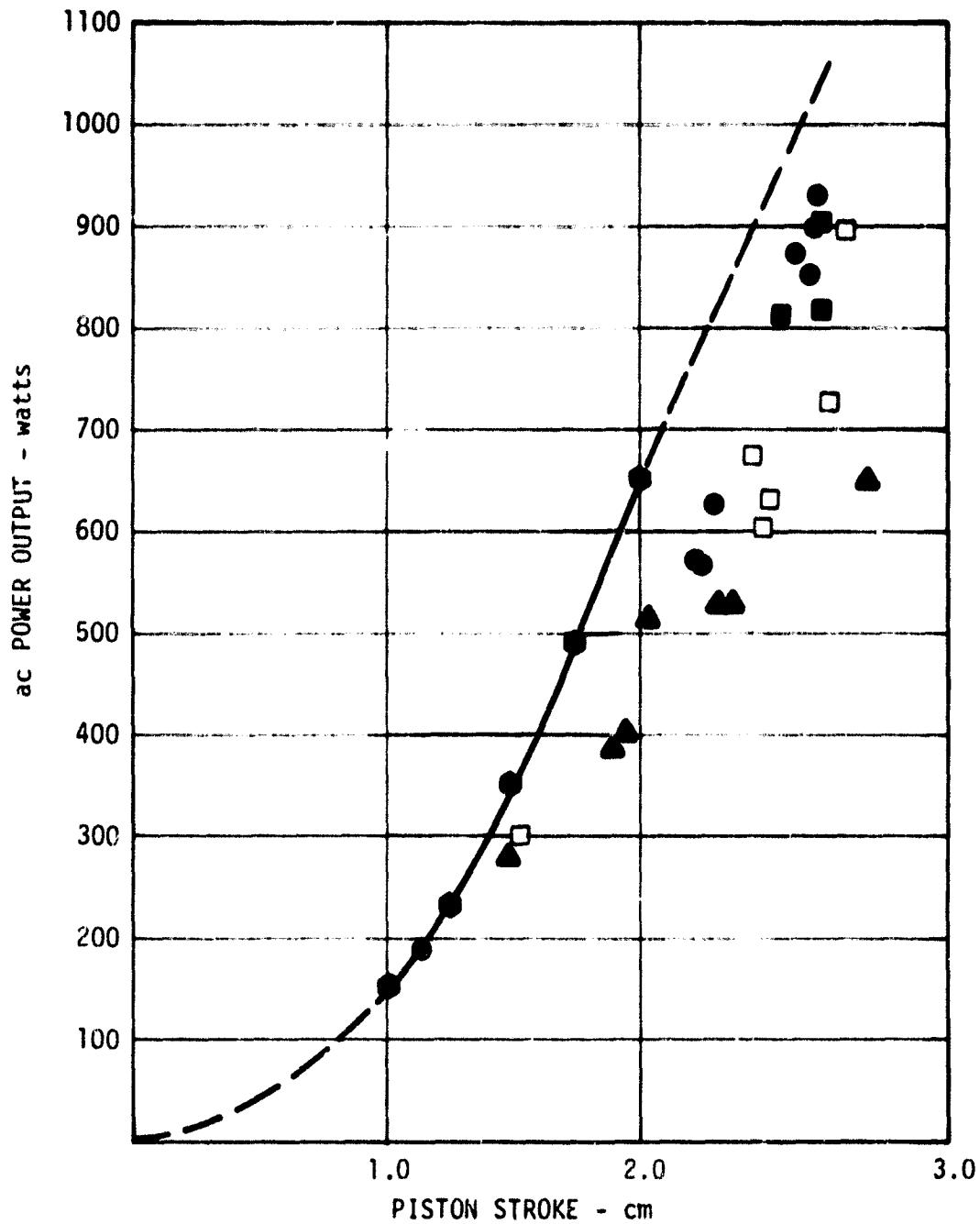
TABLE 4-3 (Cont'd)

Test Points Units	Piston Stroke cm	Engine Power W	AC Power W	Pressure bar	Displacer Stroke cm	Head Temp. °C	DC Power V	Efficiency of Engine (η_c) %	Efficiency of System (η_g) %	Frequency Hz
1/22/79 #1	1.38	37	-	40.2	1.82	160	-	6.5	-	22.9
2	1.77	59	-	40.4	2.22	177	-	7.4	-	22.9
3	2.17	87	-	40.1	2.58	197	-	7.9	-	22.9
4	2.6	123	-	40.4	2.93	216	-	8.7	-	23.0
5	1.38	103	-	59.9	1.72	193	-	10.5	-	28.0
6	1.79	169	-	60.2	2.06	213	-	11.9	-	28.1
7	2.18	226	-	60.0	2.38	233	-	12.4	-	28.1
8	2.58	297	-	60.2	2.68	259	-	12.6	-	28.2
9	1.36	55	-	69.9	1.61	220	-	4.7	-	30.2
10	1.78	127	-	69.9	1.97	245	-	7.9	-	30.2
11	2.18	163	-	69.8	2.29	262	-	7.3	-	30.2
12	2.59	174	-	70.0	2.58	294	-	6.3	-	30.3
1/29/79 #1	1.77	66	-	40.5	2.15	185	-	7.5	-	23.6
2	2.22	112	-	40.4	2.55	205	-	9.3	-	23.6
3	1.77	142	-	60.0	2.00	211	-	10.1	-	28.7
4	2.19	246	-	60.1	2.32	245	-	13.0	-	28.7
5	2.53	361	-	60.0	2.58	266	-	15.1	-	28.8
6	1.78	155	-	70.5	1.90	238	-	9.4	-	31.1
7	2.16	245	-	70.1	2.22	260	-	10.8	-	31.0
8	2.49	339	-	70.6	2.43	287	-	12.3	-	31.2

TABLE 4-5 (Cont'd)

Test Points Units	Piston Stroke cm	Engine Power W	AC Power W	Pressure bar	Displacer Stroke cm	Head Temp. °C	DC Power V	Efficiency of Engine (η_c) %	Efficiency of System (η_g) %	Frequency Hz
2/2/79 #1	.96	155	102	70.2	1.05	400	54	16.9	11.1	30.6
2	1.49	328	191	70.2	1.50	403	46	20.5	11.9	31.0
3	2.02	485	264	70.2	1.95	398	34.8	20.4	11.1	31.2
4	2.49	632	314	70.4	2.31	402	33.	20	10	31.2
5	1.11	248	174	70.1	1.16	503	186	21.1	14.8	30.3
6	1.49	381	261	70.4	1.49	506	50	20.5	14.0	30.8
7	1.96	575	385	70.0	1.85	505	55	22.7	15.2	31.0
8	2.41	728	441	70.4	2.23	485	43	22.2	13.5	32.2
9										
10	1.50	492	353	70.4	1.45	604	187	24.5	17.6	30.5
11	1.96	661	486	70.1	1.81	606	82.6	24.6	18.1	30.8
12	2.49	970	705	70.4	2.21	608	64	26.2	19.0	30.8
13										
14	1.52	437	301	69.1	1.43	664	87	21.8	15.0	30.1
15	2.02	714	515	69.8	1.86	657	71.1	24.6	17.7	30.6
16	2.49	978	707	70.3	2.16	657	72.4	26.4	15.1	30.7
17	1.13*	282	189	67.5	1.13	633	156	21.2	14.2	29.0

*Estimated



- ALTERNATOR TEST DATA 185 dc VOLTS
- FIELD VOLTAGE 150-190 dc VOLTS
- FIELD VOLTAGE 100-120 dc VOLTS
- FIELD VOLTAGE 75-90 dc VOLTS
- ▲ FIELD VOLTAGE 60-90 dc VOLTS

Fig. 4-8 1 kW Solar Engine/Alternator ac Power Output versus Stroke at 650°C and 60-80 bar

792337

System efficiency was generally between 18 and 21%. System efficiency did not meet expectations principally because of lower alternator efficiency as discussed earlier and higher-than-predicted gas spring losses. Gas spring losses were twice what was predicted. Gas spring losses will be further evaluated during testing of a sister free-piston Stirling engine/linear alternator.

5.0 CONCLUSIONS

The design, fabrication, assembly and test of the free-piston Stirling engine/linear alternator was accomplished in approximately one year. This engine/alternator system was the first system to operate both with a gas spring and at 30 Hertz, and to start by motoring the alternator. The engine/system design was based on existing hardware, but included numerous major design modifications to improve operation and reliability. The major design changes included:

- Chrome-oxide coating on critical mating surfaces
- Unibody displacer
- Posted displacer
- Gas bearings on piston

As in any developmental program, both major and minor problems arose; however, these problems were addressed and solved. The advances made on this engine have been incorporated into subsequent designs. The engine/alternator is a rugged machine, and with incorporation of a separate piston antirotational device it is also a reliable machine. The engine efficiency goal was exceeded and power output was within 10% of the nominal power requirements. Through further testing with longer stroke and/or increased frequency, the power output would exceed this value. The alternator efficiency did not reach the expected level due to fabrication problems. However, a similar alternator design has demonstrated an efficiency of 90%. Therefore, this program demonstrated that the free-piston Stirling engine/linear alternator can potentially provide high energy conversion efficiencies in comparison with other systems.

Considering the successful initial testing and characterization of the engine-alternator system, the system could be used for a solar demonstration. Prior to any solar demonstration, it is recommended that a complete engine-alternator characterization study be performed to ensure knowledgeable operation of the system when mounted to a solar collector.

Because the engine is reliable and rugged, the engine could be used in other free-piston testing programs to improve the state-of-the-art. Such testing could include:

- Operation with increased frequency
- Operation with internally supplied gas bearings
- Operation at different attitudes
- Operation with different regenerator material
- Operation with different heat input sources (including solar)

It is concluded that the objectives of the program have been marginally met and that the system is capable of meeting its intended use (i.e., demonstration of the system on a solar collector). The system represents a major improvement in the development of free-piston Stirling engine technology and, as such, should be utilized whenever additional knowledge can be derived.

APPENDIX A
TEST PLAN AND PROCEDURES

1. Assembly of engine/alternator system

- a. Receive engine from Sunpower
- b. Disassemble engine internals
- c. Assemble engine/alternator per assembly drawing 38J101 Rev. A for system hardware and per Sunpower drawing JPL 1-kW Engine for engine (Follow assembly check list procedures)
- d. Install engine displacer in engine which has a 46% larger displacer rod and an antirotational device.
- e. Assemble system assembly and housings as a unit prior to installation in engine. Power piston shaft must be prefit into system housings to ensure fit at both vertical and horizontal attitudes, and gas bearing system must be externally pressurized to ensure proper operation.
- f. Maintain cleanliness
 - all parts to be thoroughly cleaned with acceptable solvents
 - all chrome oxide parts must be cleaned with tri-chloroethylene
 - parts may be final cleaned with Freon
 - after final cleaning of all parts, parts must be protected from the environment to greatest extent possible; i.e., positive flow bench and/or bagged
 - during assembly, parts should not be touched with hands; gloves should be used
 - chrome oxide parts must not be handled directly with hands; gloves must be used
 - assembly area should be kept clean at all times and doors kept closed
- g. Perform tests which check for critical leaks; i.e., leaks from working volume to displacer interior or from working volume to bounce space.
- h. Perform piston seal leak rate test and compare with previous test results. This test will reveal unaccounted-for leak paths and provide qualitative seal quality index.

- i. Check for freedom of motion after each step of assembly of reciprocating components. After the entire assembly is complete, the reciprocating components should be oscillated by hand and by pressure pulses to ensure freedom of motion.
- j. Check all instrumentation for existence and quiescence of output.
- k. Perform visual check of system to ensure against gross problems; i.e., electrical shorts, disconnected plumbing, etc.

2. Instrumentation

- a. Attach instrumentation as listed in the test directive in parallel with assembly of engine alternator.
- b. Ensure instrumentation is attached during the assembly sequence prior to becoming inaccessible.
- c. Protect wires in power piston from vibration.

3. Check-Out

- a. Perform electrical system checks after assembly, but prior to testing, to ensure instrumentation is correct and operative.
- b. Check data reduction system and data reduction program to ensure that it is operative.
- c. Obtain calibration constants for all measurements.
- d. Identify measurements which vary from standard test parameters. Lay out data sheet which will provide for all data necessary to meet test objectives.
- e. Ensure that all expendable materials are available; i.e., helium, oscillograph paper, film.

4. Vertical Test

- a. Pressurize engine slowly, listening for leaks and watching for any unaccountable motion of the displacer or piston.**
- b. Start heating engine (may be done as engine is being pressurized).**
- c. Start cooling system after engine has over 5 bar of internal pressure. This will ensure that no water will leak inside the engine.**
- d. After the engine has reached design temperature and pressure, and with the piston unloaded, the piston and displacer can be cycled by manually adding to or discharging mass from the working gas volume.***

The rod--in-displacer design requires an initial discharge from the working gas in order to lower the pressure in the displacer gas spring. This is usually accomplished with a one-to two-second leak to atmosphere. Helium is then charged immediately into the working space, driving the displacer "on" the piston and driving the piston "out". This procedure should be continued until the engine begins to cycle.

- e. When the engine starts, the hot end temperature will decrease rapidly, so it is necessary to increase the power input.**
- f. Load down the piston as the engine power output increases to keep the amplitude of both the piston and displacer within acceptable limits.**
- g. Monitor and correct displacer and piston position, as required. This can be done manually or automatically.**
- h. Should it be necessary to stop the engine, the quickest and safest way is to expose the working gas to the bounce space volume. This brings the working gas pressure amplitude to zero and the engine stops.**
- i. Test and evaluate the following steady-state test points. The start temperature and time to reach each test point and steady operation will**

*Explanation is found at end of Appendix A.

be recorded to determine the test quantities listed below. Test points were selected to determine effect on engine performance of field current, load, and head temperature.

<u>Test Point</u>	<u>Field Current</u>	<u>Load Resist. Ω</u>	<u>Heater Temp</u>
1*	.295	55 (design)	650°F (design)
2	.2	55	650°F
3	.4	55	650°F
4	.295	45	650°F
5	.295	65	650°F
6	.295	55	550°F

j. Take nonsteady-state data at times when the engine performance is erratic or a reoccurring problem requires data for analysis and correction. Only the minimum data is taken which consists of:

1. force, pressure, power, and position plots
2. operating pressure
3. operating temperature (minimum)
4. frequency

k. Take steady-state data at times when the engine performance is consistent and there is sufficient evidence of stable energy dissipation. Adequate determination of a steady-state condition can be achieved by monitoring the power input, power output, and cooling system temperature gradient. When these have become stable over a predetermined time, the engine is considered to be in a steady-state operating mode.

Primary independent test variables are:

1. Load Demand (i.e., load resistance)
2. Field Current
3. Temperature

*All normal engine shutdowns and start-ups will be performed at point 1.

The first two variables are of primary importance for evaluating the interaction between the engine and the alternator performance. The data which will be measured or calculated at various operating conditions are:

1. Stroke
 2. Frequency
 3. Engine Power
 4. Displacer Phase & Stroke
 5. Alternator Output Power
 6. Alternator Output Voltage
 7. Alternator Output Current & Phase
 8. Output Wave Forms
 9. Heat Input
 10. Heat Rejected
 11. Power Input to Field Coil
 12. Efficiency
 13. Running Time
 14. Engine Starts
 15. Working Space Pressure Amplitude & Phase
-
- l. Log all data and observations in a concise and informative manner. This is done immediately after completion of the test to ensure the accuracy of the information.
 - m. Dismantle the engine slowly and carefully, noting any differences from the norm.
 - n. Check bearing surfaces for wear or dimensional changes.
 - o. Use the data taken during the run and the information gained from the engine inspection to evaluate the next engine test.

*A more desirable method on engine starting was developed during the initial test phase of the JPL Stirling engine-linear alternator. The engine was brought to an intermediate temperature of -250°C . At this point the dynamic components of the engine were driven, using the alternator as a motor. Power was generated by a sine wave generator through a power amplifier to the motor/alternator. Field voltage on the alternator, set initially at design conditions, was slowly reduced while monitoring the alternator power input voltage and current phase relationship. When the field current was reduced to a power where the current and voltage phase was indicative of zero power transfer, the amplifier was switched off and the engine operated on its own.

This start procedure resulted in a smooth, steady, predictable start sequence and eliminated the possibility of overstroking the engine while power and load were being matched as is done in the "blip" start method.